Effect of Urban Environmental Stress on Tree Vitality, Mycorrhiza and Root Morphology of Roadside *Tilia sp.*

Dylan Goff BSc.

Supervisors: **Priv.-Doz. Dr. Hans Sandén**

Assoc. Prof. Dipl.-Biol. Dr.rer.nat. Boris Rewald

Contents

Introduction

Trees in urban areas face numerous adverse conditions such as poor soil, de-icing salt, air pollution, vandalism, drought, elevated summer temperatures, and frost damage (Pauleit et al. 2002). They are frequently restricted in their root zones and urban soils are often compacted with less soil porosity than forest soils (Tyburska et al. 2013). While incurring the various strains caused by conditions in the urban environment, green areas and vegetation provide numerous ecosystem services in cities and towns, such as mitigating urban "heat island effects" by blocking the absorption of short wave radiation by sealed surfaces via shading, but by evaporative cooling during evapotranspiration (Taha 1997, Kuttler 2011). These sealed surfaces are often built from materials with a low albedo, which absorb short wave radiation and emit this radiation as heat energy, increasing the air temperature in urban areas (Taha 1997). Urban vegetation also plays an important role in filtering urban air and removing harmful pollutants such as SO_2, CO and NO_x (Jim and Chen 2008, Arantes et al. 2019). In addition to these ecosystem services, urban trees have also been linked to better physical health and better mental health amongst urban populations (Nowak et al. 2013, Taylor et al. 2015). Urban trees therefore play an important role in buffering the many negative impacts of urban conditions on people in cities and towns. *Tilia sp.* are commonly used as an urban tree in Europe (Timonen and Kauppinen 2008). They are large trees with dense foliage that grow well in semi-shaded places, they provide food sources for insects and have a low allergy potential, giving them desirable qualities for the urban environment (Dresden 2015). They have good late frost tolerance and medium heat tolerance and can also moderately tolerate soil compaction, although they are sensitive to waterlogging and drought conditions (Dresden 2015). However, *Tilia sp.* have a low salt tolerance, and absorb more Na+ ions per leaf area than many plants with smaller leaves (Kleiber et al. 2019).

Urban soils can also be extremely heterogeneous in terms of physical and chemical composition, as the result of human activity over centuries of settlement in urban areas (Karliński et al. 2014). Salt damage from road de-icing salts is a problem for trees in urban areas (Bryson and Barker 2002). Sodium and Chlorine from de-icing salts spread in winter enter urban soils and are taken up by trees in the spring along with water as the rate of transpiration increases (Bryson and Barker 2002). Salinity is known to negatively affect water absorption in plants, due to a quick osmotic phase which leads to physiological drought effects in plants (Schiop et al. 2015). The negative effects of salt application on tree vitality generally decreases with increasing distance from roads (Bryson and Barker 2002), and more salt is applied on streets with heavier traffic (Sucoff 1975). Cl- is readily absorbed by plants, and accumulates in leaves where it has a negative effect on leaf tissue (Czerniawska-Kusza et al. 2004). Na^+ remains in soils for longer than Cl^- because it is positively charged and is not repelled by the negatively charged soil colloids, unlike the negatively charged Cl^- (White and Broadley 2001). This makes Na^+ a good parameter for determining salt stress in urban soils. Na^+ ions from de-icing salts

can wash out Ca^{2+}, Mg^{2+} and K^{+} and displace soil particles, resulting in reduced permeability and lead to increases in the sodium share of the cation exchange capacity (CEC) in urban soils at the expense of the other cations (Norrström and Bergstedt 2001, Cunningham et al. 2008, Asensio et al. 2017). Leaching of base cations can also result in the displacement of heavy metal ions, often into water systems (Bäckström et al. 2004). Urban soils contain high amounts of calcium due to deposition from fine particles and weathering of calcium rich building materials, often resulting in higher soil pH levels (Li et al. 2013). This alkalisation of urban soils by $CaCO_3$ can have a negative effect on plants by reducing the availability of phosphorous and micronutrients (Kleiber et al. 2019). Urban trees must often cope with this myriad of stresses simultaneously, and the strain induced from one type of stress may leave them vulnerable to incurring physiological strain from other forms of stress, making loss of vitality in urban trees a complex situation (Urban 2008).

Mycorrhizal fungi are fungi that form a mutualistic symbiotic relationship with plants, whereby water and nutrients are transported to the plant in exchange for photosynthetically produced sugars (Tyburska et al. 2013). Mycorrhizae are also thought to benefit trees by helping mitigate drought effects, for example by increasing aquaporin expression in roots, and by providing an extension of the root absorbing surface area - especially in long distance exploration types of mycorrhizae – although this is debated (Lehto and Zwiazek 2011). Mycorrhiza can also potentially help the host tree withstand salt stress by increasing mineral nutrition to compensate for nutrient displacement in soils by Na^{+}, improving the water status of trees, and reducing the amount of salt the tree absorbs (Weissenhorn et al. 2002). Mycorrhizae have also been shown to help trees maintain growth under salt stress conditions by alleviating the need to invest C in the maintenance of cell functioning (Rewald et al. 2015). While mycorrhizae benefit urban trees in mitigating urban stresses, mycorrhiza in urban areas themselves face numerous stress factors (Tyburska et al. 2013). Salt stress, high soil acidity, habitat fragmentation, nitrogen enrichment, heavy metal pollution, drought, and a reduced allocation of photosynthates when poor tree health results in chlorosis or casting of leaves, may each play a part in preventing adequate colonisation of root tips by mycorrhizae in urban trees (Dixon et al. 1993, Newbound et al. 2010, Tyburska et al. 2013). *Tilia sp.* found in forests typically form ectomycorrhizal (EcM) associations with up to 10 – 15 EcM species (Lang et al. 2011). However, urban *Tilia* trees often host far fewer colonizing species than their forest counterparts (Timonen and Kauppinen 2008). This may result in a disadvantage for urban Tilia sp. trees in adapting to urban stresses, as the abovementioned mitigating effects provided by some species of mycorrhiza may be absent. While much research has been done on the aboveground vitality of urban trees, there are only a few studies exploring the impact that soil conditions have on urban *Tilia sp*. and the interplay between those soil conditions, mycorrhizae and the trees themselves.

Aim and Hypothesis

The prominence of *Tilia sp.* as a street tree species in Central Europe make it an important tree to research concerning vitality. Despite this, not much research has been carried out on the root zones of urban *Tilia sp.* trees in Central Europe. The aim of this paper is to look at belowground biological parameters that may explain the health status of *Tilia sp.* street trees in Vienna, compared to healthier park trees – in particular the interplay between salt, mycorrhiza and tree health. To do so we measured aboveground vitality and belowground biological and chemical parameters (soil chemistry, base saturation, microbial biomass, mycorrhizae) of *Tilia sp.* from parks (no de-icing salt application), side streets (moderate de-icing salt application), and main streets (heavy de-icing salt application).

We hypothesise that:

1. Soil Na^+ content increases with increasing urban stress.
2. Na^+ application of de-icing salts results in nutrient imbalances in soils.
3. Increasing soil Na^+ levels have a negative relationship with tree vitality.
4. Deceased ectomycorrhizal colonization of *Tilia sp.* root tips will coincide with decreased aboveground tree vitality.

Materials and methods

Study area

Trees for the study were chosen from a GIS grid from parks and streets across northern and western Vienna, Austria in spring 2017. In total, 60 *Tilia sp.* trees were chosen by locations relative to their exposure to de-icing salt applications, 20 in main streets (assumed to be subjected to heavy stress), 20 in side streets (assumed to be subjected to moderate stress), and 20 in parks (control). The exact species of *Tilia* is often difficult to determine in European cities due to hybridisation (Weryszko-Chmielewska et al. 2019).

Bachelor students studying Environmental Science selected trees as part of a related thesis. Certain criteria were taken into account in the course of choosing trees for the study – planting pit shape and size, pit border parameters (height of curb and potential for water run-in), visibility of compaction or soil elevation, sealing of surfaces, distance to buildings and solar radiation – in order to allow the trees to be comparable.

Above Ground Vitality

Trees were assessed for above ground vitality by the bachelor students according to guidelines taught to them by representatives of the Vienna municipality MA 42 (Table 1). Trees were allocated a vitality score between 1 and 10 depending on vitality criteria.

Table 1. Above ground vitality scores and criteria for urban trees according to Vienna municipality.

Vitality score	Criteria
10	Fully vital, healthy tree with no chlorosis or dieback
9	No dieback, no visible parasites (e.g. mistletoe species), no chlorosis, dense crown (sky not visible from below in full flush), no visible disease on trunk. Not as dominant as 10 in terms of height at same age
8,7,6	*In relation to 5 and 9*
5	Mild dieback of crown, no chlorosis, medium crown density (50% of sky visible from below in full flush)
4,3,2	*In relation to 1 and 5*
1	>70% dieback of crown, visible parasite infection (e.g. mistletoe species), chlorotic and necrotic leaves, sparse crown, visible stem disease.

Figure 1 Stressed *Tilia sp.* from a main street site (left) and a vital *Tilia sp.* from a park site (right)

Mycorrhizal in-growth bags

Triangular shaped bags measuring 7 x 6 x 6cm were fashioned from nylon mesh (PA – 50/37, Art 10167/1020, Franz Eckert GmbH, Waldkirch, Germany) and filled with 14g sand. They were sealed and strings were attached using a Rotek PM-FS-400-S impulse laminator (Rotek GmbH, Hagenbrunn, Austria). The bags were buried in May 2017 at a depth of 10 to 15 centimetres at a distance of 50 to 60 cm from the sample trees. The position of each bag was noted to avoid the accidental harvesting of the in growth bags during soil coring. Bags were harvested in October 2017. In growth bag colonization by mycelia was assessed visually under a Zeiss Erc5s Axiocam camera on a Zeiss Stemi 2000-CS microscope (Carl-Zeiss AG, Oberkochen, Germany) according to a scale from 0 to 4 (Wallander et al. 2001):

0	No mycelia present
1	Sparse mycelia present
2	Mycelia present but no aggregation of the sand particles
3	Plenty of mycelia present and some aggregation of the sand particles
4	Plenty of mycelia present and sand particles aggregated to a great extent

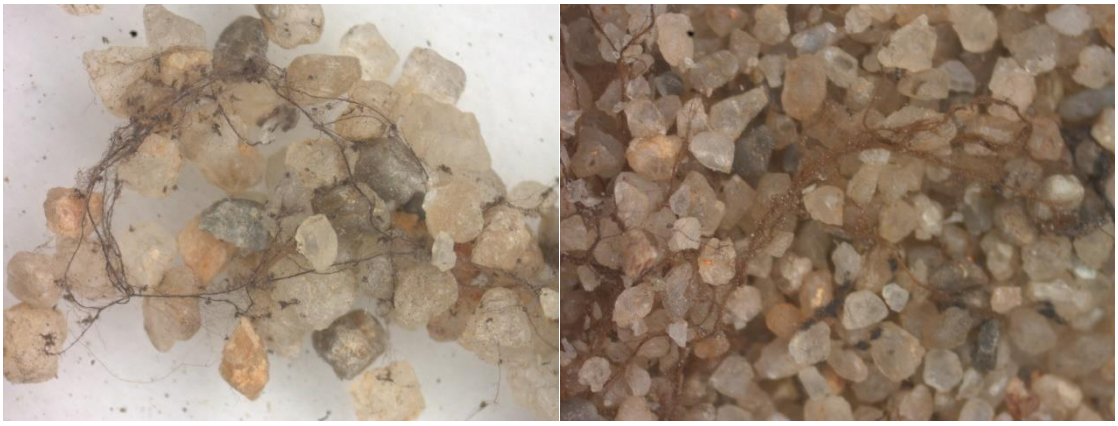

Figure 2 Microscope images of rhizomorphs (left) and mycelia (right) as observed in ingrowth-bags.

Root and soil sampling

One core was collected at a distance of 50cm to 60cm from each sample tree in July 2017 to a depth of 50cm where possible, using cores with 6.8cm diameter, and refrigerated at 6°C in polystyrene containers for no longer than 3 weeks until processing. The distance from the top of the core to the soil surface was measured during collection, both on the inside and on the outside of the corer, in order to compensate for compaction during the coring process and accurately assess soil depth. In October 2017, soil samples from a depth of 15 -20cm were taken at a distance of 50 to 60cm from each tree simultaneously to harvesting of in-growth bags.

Figure 3 Example of a core taken from one of the sample trees

Core processing

Cores were opened within three weeks of sampling in July 2017, measured into segments of 0 – 10 cm, 10 – 30 cm, and 30 – 50 cm. The 0 – 10 cm and 30 – 50 cm segments were wet sieved to remove roots. Roots from these segments were divided into living and dead roots, and stored at 40°C until

weighing.

The 10 – 30 cm root segments were carefully dry sieved to preserve spores from mycorrhizae and to avoid damaging the ectomycorrhizal mantels on the fine roots. The roots were rinsed carefully and scanned in an Epsom Expression 10000 xL scanner (Seiko Epson Corporation, Nagano, Japan). Number of root tips, root lengths, and root diameters and measured using WinRHIZO^{TM} software (Regent Instruments, Quebec City, Canada). Three or four root segments were then selected for analysis of Ectomycorrhizal colonization rate and morphotyping. After analysis of roots for ectomycorrhizal colonisation (see below), all roots were dried and weighed.

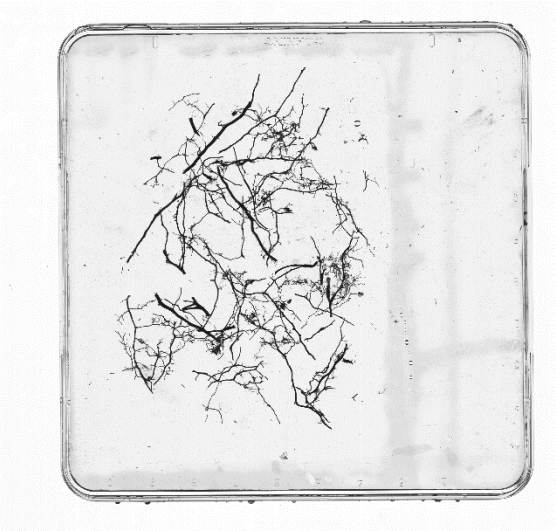

Figure 4 Example of a scan of roots from 10 – 30cm soil depth, scanned with Epsom Expression 10000 xL scanner

Mycorrhizal Colonisation

Root segments were magnified using a Zeiss Axiocam camera on a Zeiss Stemi 2000-CS microscope (Carl-Zeiss AG, Oberkochen, Germany).

Mycorrhizal colonisation rate was determined by counting 150 root tips per tree where possible, and noting the presence or absence of an Ectomycorrhizal (EcM) mantel. Differences in EcM mantel morphotypes were determined and they were categorized, whereby differences in mantel length, colour, hairiness, surface texture and shape were taken into account.

Figure 5 Ectomycorrhizal root tips from *Tilia sp.*

Morphotypes were quantified as the number of distinct morphotypes per sample. Simpson indices for morphotypes were calculated between treatment types (Equation 1):

EQUATION 1: SIMPSON INDEX OF ECM MORPHOTYPES

$$D = 1 - \sum_{i=1}^{R} p_i^2$$

Where p_i is the proportion (n/N) of each morphotype to the total number of morphotypes found.

Enzyme analysis

We attempted to analyse soil enzymes from all samples. However, because of extreme heterogeneity of the soil samples, quenching calculations were impossible and we were unable to produce any meaningful results. A description of the methods employed in enzyme analysis can be found in the appendix, but we are unable to present any results in this paper.

Microbial Biomass Carbon and Nitrogen

Microbial biomass carbon and nitrogen were measured using the fumigation extraction method (Jenkinson and Powlson 1976). Two sets of 5g fresh soil from 10cm to 30cm soil depth, collected in October 2017, were sieved to 2mm. One set was fumigated in a desiccator for 24 hours, using $CHCl_3$ to exterminate soil microbes. One set of soil samples was left unfumigated. The C and N from the

samples were then extracted in 25ml K_2SO_4 and filtered. The filtered samples were analysed using the Shimadzu TOC-L Total Carbon Analyser and TNM-L Nitrogen Analyser (Shimadzu Corporation, Kyoto, Japan) to determine the amount of Carbon and Nitrogen present in the samples. The Microbial Biomass was calculated as the difference between fumigated and non-fumigated samples, with a correction factor of 0.45 for carbon and 0.54 for nitrogen (Joergensen 1996, Joergensen and Mueller 1996). This correction factor is necessary because not all microbial carbon and nitrogen is extracted in the method:

EQUATION 2: MICROBIAL BIOMASS N $$\text{MICROBIAL BIOMASS N} = E_N/k_{EN}$$

Where E_N = N extracted from fumigated soil minus N extracted from non-fumigated soil, and k_{EN} = extractable N from microbes after fumigation (=0.54). Microbial biomass C was also calculated in a similar way:

EQUATION 3: MICROBIAL BIOMASS C $$\text{MICROBIAL BIOMASS C} = E_C/k_{EC}$$

Where BC = C extracted from fumigated soil minus C extracted from non-fumigated soil, and KEC = extractable C from microbes after fumigation (=0.45).

Total Carbon and Nitrogen

250mg of soil collected in October 2017 (sieved to 2mm and dried at 105°C for 24h) were weighed inside enclosed tin capsules and stored in an autosampler. A linear standard calibration curve was created with certified sample material. The samples were then combusted under a constant oxygen stream at 950°C, CO_2 and NO_x were determined via infra-red detection using a Leco Truspec CN analyser (Leco Corporation, St. Joseph, Michigan, USA) for carbon and thermal conductivity for nitrogen. Results were expressed as grams of carbon / nitrogen per 100g soil. Inorganic and organic carbon were not differentiated in this experiment.

Soil pH

Soil pH was measured from fresh soil samples collected in October 2017. Two sets of 5g fresh soil were shaken in 0.01 Mol $CaCl_2$ and in 25ml deionized water respectively. The slurry was allowed to rest for over 2 hours before measurement with a Schott pH-meter CG840 (Schott Instruments GmbH, Mainz, Germany).

ICP Analysis

2.5 g dry soil from samples collected in October 2017 was extracted for 24h in 50ml ammonium acetate at 1 molar concentration with deionised water, filtered and the filtrate was analysed using a PerkinElmer® Optima™ 8300 Optical Emission Spectrometer (Perkin Elmer Inc., Waltham, MA, USA). Soils were measured for aluminium, arsenic, boron, calcium, cadmium, copper, iron, mercury, potassium, magnesium, manganese, molybdenum, sodium, nickel, phosphorous, lead, sulphur, and zinc. These values were delivered in µg / g dry soil for trace elements, and in mg/g dry soil for macronutrients such as Calcium, Magnesium, and Potassium. Where levels were below the detection value, a value of 2/3 the minimum detection value was assigned for statistical analysis.

Cation Exchange Capacity (CEC) was calculated by converting the ppm value for K^+, Ca^{2+}, Mg^{2+}, Na^+, Fe^{2+}, Al^{2+} to $\mu mol_c/g$ values. H^+ values were derived from pH levels, and the CEC was calculated as the sum of these cation values (Equation 4).

EQUATION 4: CATION EXCHANGE CAPACITY

$$\boldsymbol{CEC = K^+ + Ca^{2+} + Mg^{2+} + Mn^{2+} + Fe^{2+} + Al^{2+} + Na^{2+} + H^+}$$

Base saturation was calculated as K + Ca + Mg+ Na given as a percentage of CEC (Equation 5).

EQUATION 5: BASE SATURATION

$$\boldsymbol{BS\% = \frac{K^+ + Ca^{2+} + Mg^{2+} + Na^+}{CEC} x\,100}$$

To examine the relationship of the major cations to each other, each base cation ($\mu mol_c/g$) was calculated as a percentage of the total of all four base cations extracted (see equations 6,7,8,9).

EQUATION 6: NA%

$$Na\,\% = \frac{Na^{+}}{Na^{+} + Ca^{2+} + K^{+} + Mg^{2+}} x100$$

EQUATION 7: CA%

$$Ca\,\% = \frac{Ca^{2+}}{Na^{+} + Ca^{2+} + K^{+} + Mg^{2+}} x100$$

EQUATION 8: MG%

$$Mg\,\% = \frac{Mg^{2+}}{Na^{+} + Ca^{2+} + K^{+} + Mg^{2+}} x100$$

EQUATION 9: K%

$$K\,\% = \frac{K^{+}}{Na^{+} + Ca^{2+} + K^{+} + Mg^{2+}} x100$$

Statistical Analysis

Statistics were analysed using R Studio (RStudio Team (2015). RStudio: Integrated Development for R. RStudio, Inc., Boston, USA). Outliers (samples greater or less than 2 times the standard deviation from the mean) were removed. Kruskal- Wallis and Dunn's tests were used to analyse differences between treatment levels (main streets, side streets, parks), as ANOVA assumptions of normally distributed residuals and homogeneity of variances were not met. Correlations between parameters were analysed via Spearman tests.

Results

Tree Vitality

Tilia sp. trees in the control plots had the highest vitality, whereas trees on the main streets had the lowest vitality, all locations were significantly different from each other (Figure 6).

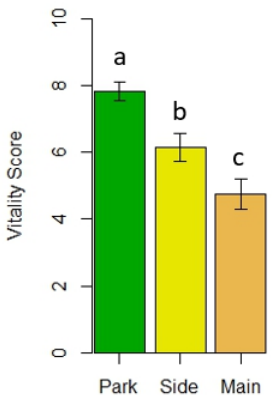

Figure 6 Mean vitality scores for Viennese street trees for samples from parks (n=20), side streets (n=20) and main streets (n=20).

At 0 - 50cm soil depth, living root biomass tended to be higher in the streets than in the parks (figure 7A). This pattern was also present at 10 – 30 cm depth (figure 7B), and at 30 – 50 cm depth (figure 7D). In the 10 – 30 cm soil depth, where we also measured mycorrhiza and root morphology, the root biomass in side streets was significantly higher than both park and main streets (figure 7C). The high root biomass in the side streets at 10 – 30 cm depth resulted in low SRA and SRL measurements (figure 7G and 7H), and indicate a high root density in side streets at this depth (figure 7I). This pattern was not reflected in root tips/cm (figure 7E) or mean root diameter (figure 7F), which were both similar for all locations at 10 – 30 cm depth.

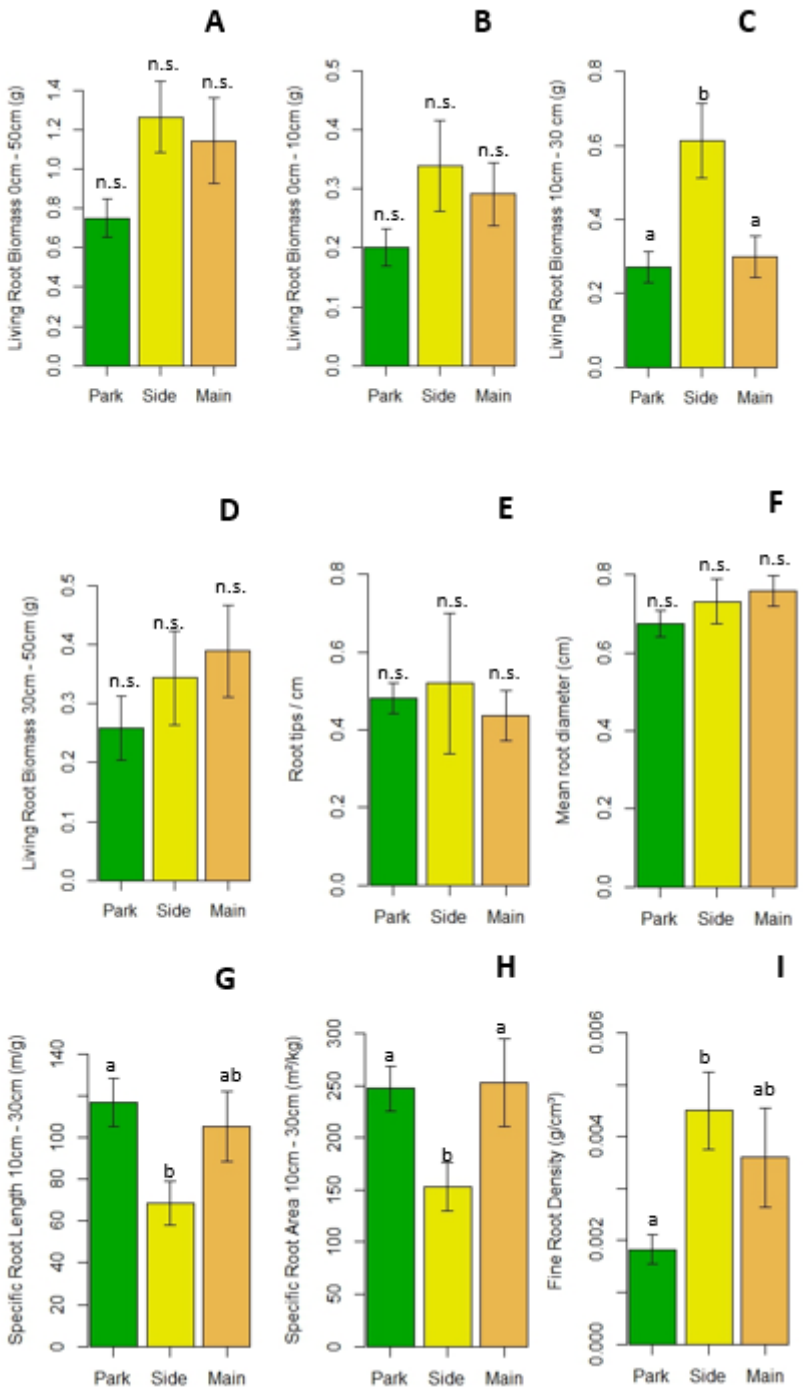

Figure 7 Root parameters for *Tilia sp*. trees in parks (n=20), side streets (n=20) and main streets (n=20). **7A** shows mean living root biomass from 0 – 50cm. **7B, 7C, 7D** breaks the living root biomass into 0 – 10cm, 10 – 30cm and 30 – 50cm depths respectively. **7E** shows number of root tips / cm at 10 – 30cm depth. **7F** shows mean root diameter for roots <2mm at 10 – 30cm depth. **7G** and **7H** show Specific Root Length and Area respectively, **7I** shows the root density at 10 -30cm (g roots per cm^3 soil**)**

Soil Chemistry

Exchangeable soil sodium (Na µg/g) tended to increase with increasing urban stress, although sodium levels in side and main streets did not differ significantly (Figure 8A). Cation exchange capacity remained similarly high between locations (Figure 8B). Similarly, base saturation (not pictured) was around 99.7% for all three groups with no significant differences.

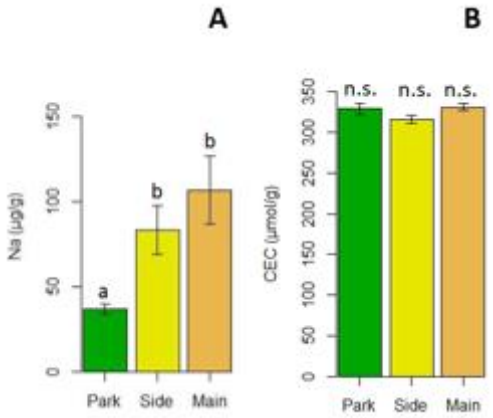

Figure 8 Mean soil Na (µg/g) in Viennese street tree planting pits for samples (N=60) from parks (n=20), side streets (n=20) and main streets (n=20) at a depth of 10-30cm.

In contrast to sodium, exchangeable soil magnesium was higher in the parks than in streets (figure 9C). Values for soil exchangeable calcium were similar across all locations, and greatly exceeded the values for the other cations (figure 9A). Potassium and phosphorus were also similar in all locations (figure 9B and 9D).

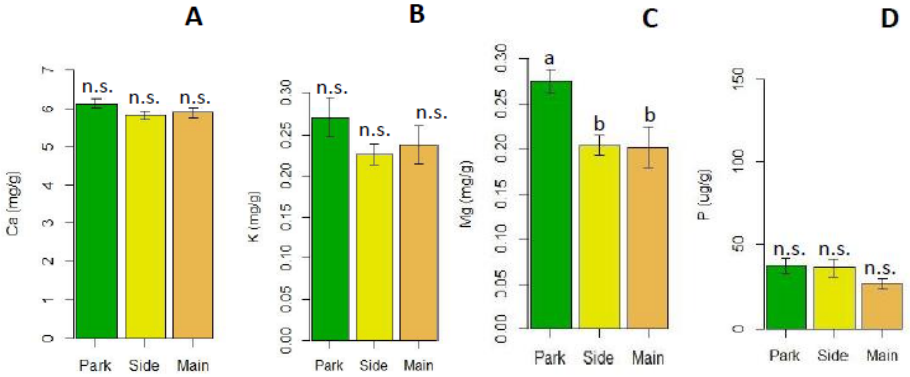

Figure 9A Mean soil Ca (mg/g) in Viennese street tree planting pits for samples (N=60) from parks (n=20), side streets (n=20) and main streets (n=20). **B** shows the mean K (mg/g) levels. **C** shows the mean Mg (mg/g) levels. **D** shows the mean P (µg/g) levels. All figures were measured at a soil depth of 10 – 30cm.

The percentages of total base cation concentrations occupied by each cation showed differences for Na% and Mg% (Figure 10). Like Na (µg/g), exchangeable Na% was lowest in park soils with no significant differences between street soils (figure 10C). Exchangeable Mg% showed the opposite pattern and had significant differences between all three locations (Figure 10D). On the other hand,

exchangeable Ca% (Figure 10A) and K% (Figure 10B) showed no differences between locations. Ca^{2+} was dominant in all locations, comprising around 90% of the base cations found in the soils.

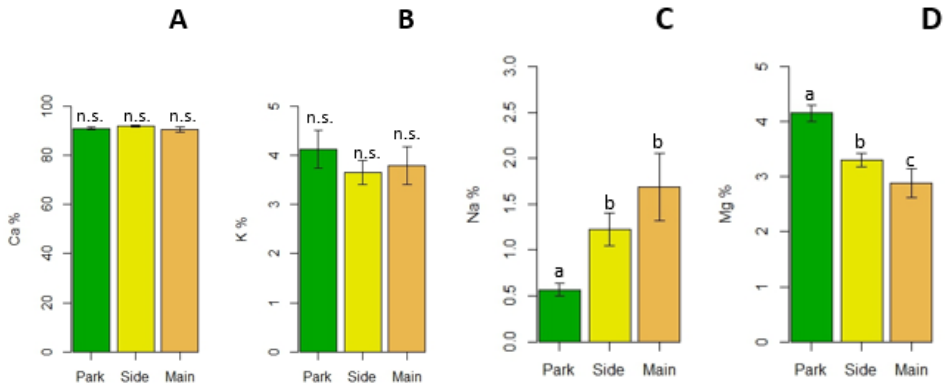

Figure 10A Percentage of the four major cations soil cations (Ca, K, Mg, Na) occupied by Ca. **B** Percentage of cations occupied by K. **C** Percentage of cations occupied by Na. **D** Percentage of cations occupied by Mg. Only Na% and Mg% showed differences between groups. Mg% was highest in the parks, Na% was lowest in the parks.

The ratio of Ca : Na in the street groups were only about half the values of those in the parks (Figure 11A). The K : Na ratio (Figure 11B) and Mg : Na ratio (Figure 11C) showed similar patterns. The P : Na ratio was highest in the parks and lowest in the main streets, but neither group showed any difference to the side street group (Figure 11D).

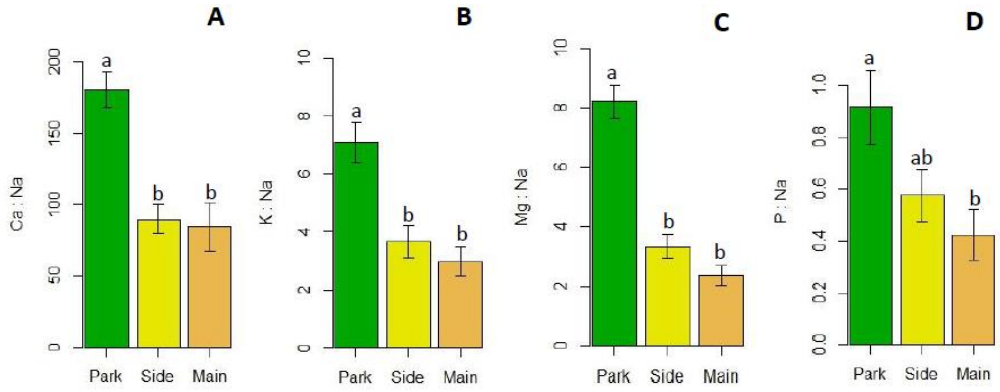

Figure 11A Mean soil Ca : Na in Viennese street tree planting pits for samples (N=60) from parks (n=20), side streets (n=20) and main streets (n=20). **B** shows the mean K : Na ratio. **C** shows the mean Mg : Na ratio. **D** shows the mean P : Na ratio. All figures were measured at a soil depth of 10 – 30cm

The Ca to Mg ratio (Figure 12A) was lowest in the parks and highest in the main streets and had significant differences between parks and the two street locations. In contrast, Ca : K, Mg : K, P : K, and P : Mg ratios showed no significant differences between locations (Figures (12B – 12E).

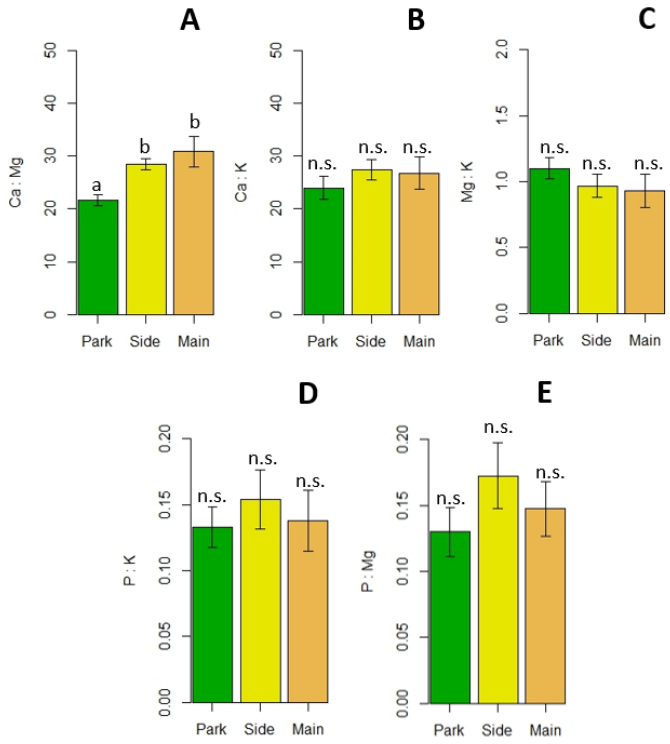

Figure 12: Mean ratios of exchangeable soil cations. **A** Calcium to Magnesium ratio. **B** Calcium to Potassium ratio. **C** Magnesium to potassium ratio. **D** Phosphorus to Potassium ratio. **E** Phosphorus to Magnesium ratio.

However, Dissolved Organic Nitrogen (DON) was higher in parks and side streets than in main streets (Figure 13A). Mean pH values after extraction with $CaCl_2$ were 6.7 in parks and side streets and 6.8 in main streets with no significant differences between groups (Figure 13B).

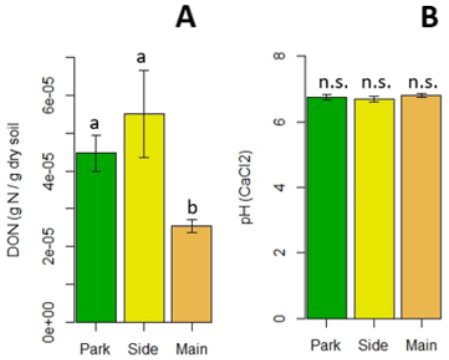

Figure 13A shows the mean Dissolved Organic Nitrogen (DON) for each group at a depth 10 – 30cm. **B** shows the mean pH measured with $CaCl_2$ for each treatment group.

Cadmium tended to increase with increasing exposure to urban conditions (Figure 14A). In contrast to this, Hg^{2+} in park soil was higher than in side and main street soils (Figure 14C), which was similar to the pattern shown by soil magnesium. Copper did not show a trend, nor did it differ according to location (figure 14A)

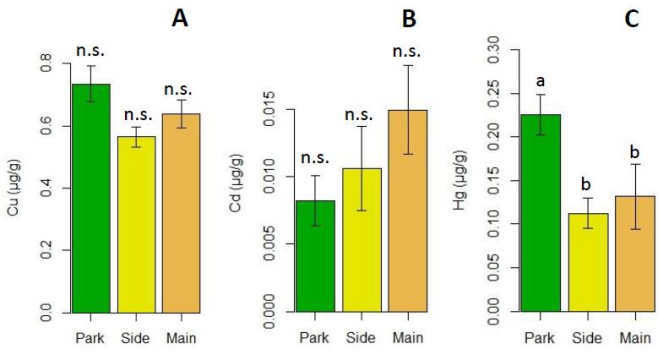

Figure 14A Mean soil Cu (µg/g) in Viennese street tree planting pits for samples (N=60) from parks (n=20), side streets (n=20) and main streets (n=20). **B** shows the mean Cd (µg/g) levels. **C** shows the mean Hg (µg/g) levels. All figures were measured at a soil depth of 10 – 30cm

Mycorrhizae and Soil Microbes

The percentage of root tips colonised by ectomycorrhizae decreased with increasing exposure to urban conditions (Figure 15A). Despite the higher colonization in parks, the number of mycelia found in in growth bags was far lower in park soils than either of the street tree soil groups (Figure 15B). This was partly due to the number of rhizomorphs: almost no rhizomorphs were found in the in growth bags from the parks – 1 bag out of 15 bags harvested, while side and main streets had rhizomorphs in 8 bags (from 14 harvested) and 7 bags (from 11 harvested) respectively. The number of morphotypes between groups also tended to decrease with increasing urban stress (Figure 15C). The Simpson diversity index for morphotypes had no great differences, ranging from 0.874 in parks to 0.844 in side streets, main streets had an index of 0.864.

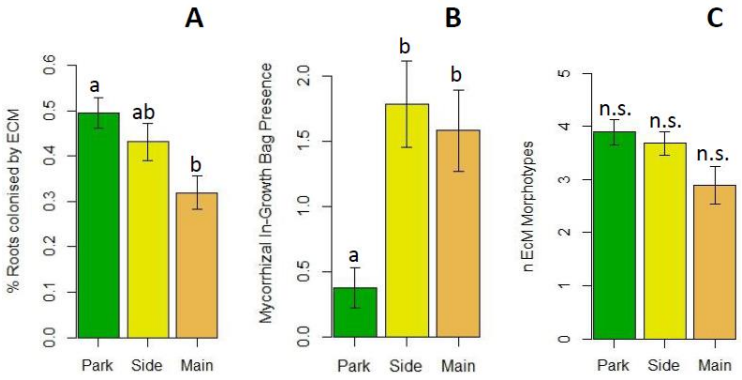

Figure 15A Mean proportion of root tips colonised by EcM (n colonised root tips/150 root tips) in Viennese street tree planting pits for samples from parks (n=20), side streets (n=20) and main streets (n=20). **B** shows the mean scores on the scale for mycelia found in-growth bags (Scale 0 – 5: 0 = no mycelia, 1= very rare occurrences, 2= some mycelia everywhere but no aggregation, 3 = aggregates present, 4= aggregates large and abundant, 5 = single large inseparable aggregate). **C** shows the mean number of EcM morphotype per sample. All figures were measured at a soil depth of 10 – 30 cm

Microbial carbon tended to be highest in side streets, in a similar pattern to root biomass (Figure 16A). Microbial nitrogen was similar in all locations (Figure 16B). Despite the differences in microbial C, microbial C : N did not differ between locations (Figure 16C).

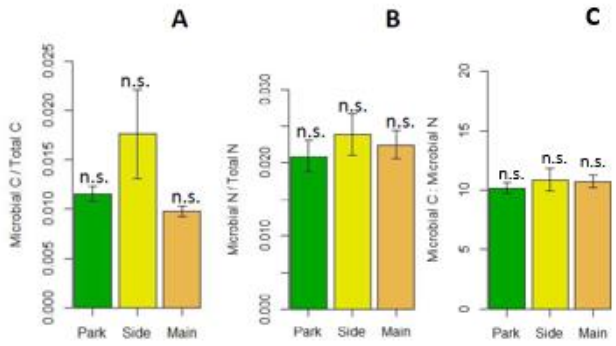

Figure 16A Mean microbial biomass carbon, as a proportion of total carbon, extracted via fumigation extraction method from Viennese street tree planting pits for samples from parks (n=20), side streets (n=20) and main streets (n=20). **B** shows the mean microbial biomass nitrogen as a proportion of total nitrogen. **C** Microbial C:N ratio. All figures were measured at a soil depth of 10 – 30cm.

Correlations

Vitality

Street tree vitality had a negative correlation with Na (µg/g), Na%, and Cd (µg/g) (Table 2A, Table 5). It was positively correlated with all ratios of macronutrients to sodium (Mg/Na, Ca/Na, K/Na, P/Na), whereby Mg/Na was the strongest (Table 6). This coincided with positive correlations between vitality and Mg, and with Hg (Table 2A). Vitality also had a negative correlation with the number of mycelia found in in-growth bags (Table 3).

Root Biomass

The mass of vital roots (< 2mm diameter) found in cores produced a negative correlation with K (mg/g), and negative correlations with base saturation, and Cu (µg/g) (Table 2A). There was a negative correlation between vital root mass and the number of root tips per sample, and a negative correlation with the number of ectomycorrhizal morphotypes per sample (Table 3). There were no correlations between above ground vitality of *Tilia sp*. and root biomass at any soil depth.

Root Tips

Number of root tips per sample and number of morphotypes were positively correlated (Table 3).

Ectomycorrhizal Colonization

The percentage of root tips colonized by ectomycorrhizae was positively correlated with Ca/Na, K/Na, and Mg/Na ratios (Table 6). This coincided with a positive correlation between colonization percentage and magnesium (Table 3), and a tendency towards a negative correlation with Na (Spearman rho -0.25, p=0.075).

In-Growth Bag Mycelia

The number of EcM mycelia found in the in-growth bags were negatively correlated with K (µg/g), P (µg/g), Base Saturation (Table 2A), K/Na, P/Na and Mg/Na ratios (Table 6) and with Dissolved Organic Nitrogen (Table 3). Mycelia and Cadmium were positively correlated (Table 2A), as were mycelia and microbial nitrogen (Table 3).

Ectomycorrhizal Morphotypes

The number of ectomycorrhizal morphotypes per sample (150 root tips per tree) was positively correlated with Mg (mg/g), and negatively correlated with Cu (µg/g) and with cation exchange capacity (Table 2A).

Magnesium (mg/g)

Soil Mg (mg/g) was strongly correlated with Hg (µg/g) (Table 2B). Mg (mg/g) was also positively correlated with Ca (mg/g) had a moderate positive correlation (Table 2B).

Exchangeable Cation Percentages

Across all samples, Ca% (the percentage of Na + Ca + Mg + K occupied by Ca) was negatively correlated with Na%, Mg% and K% respectively, and these correlations were most pronounced in main street sites with the exception of K% which was more negatively correlated to Ca% in parks (Table 4). There was no relationship between Na% and K% across all samples, but there was a positive correlation between these percentages in the park soils (Table 4). Exchangeable Mg% was positively correlated to aboveground tree vitality, EcM colonization rate and number of morphotypes per sample (Table 5). It was negatively correlated to mycelia. Exchangeable soil Na% (percentage of base cation concentration occupied by Na^+ – see methods) was negatively correlated to vitality (Table 5).

Cation Ratios

Table 6 shows correlations between soil cation ratios and biological parameters. Vitality had a positive relationship with soil Ca : Na, K : Na, Mg : Na and P : Na ratios. It was negatively correlated with the soil Ca: Mg ratio, as were number of root tips. Mycelia were positively correlated with soil Ca : Mg, Ca : K, Ca : P ratios, and negatively correlated to K : Na, Mg: Na and P : Na ratios. Ectomycorrhizal colonisation was positively correlated with soil Ca : Na, K : Na and Mg : Na ratios, but negatively correlated to Ca : Mg and K : Mg ratios. Number of ectomycorrhizal morphotypes was positively correlated to soil Mg : Na and P : Na ratios, but negatively correlated to soil K : Mg ratio. Fine root biomass at 10 – 30 depth was positively correlated to Ca : K and Mg : K ratios

Table 2A Spearman correlations for vitality, vital root mass, n root tips, mycorrhizal colonization, in-growth bag mycelia, n EcM morphotypes, Microbial N and C and Mg (mg/g) and the soil chemistry parameters measured via ICP. CEC = cation Exchange Capacity, BS = Base Saturation. All figures were measured at a soil depth of 10 – 30cm

	Vitality	Root Biom.	Root Tips	EcM Col.	Mycelia	Morphotypes
Al ug/g	NS	NS	NS	NS	NS	NS
Ca mg/g	NS	NS	NS	NS	NS	NS
Cd ug/g	-0.43**	NS	NS	NS	0.33*	NS
Cu ug/g	NS	-0.29*	NS	NS	NS	-0.29*
Hg ug/g	0.36**	NS	0.31*	NS	NS	NS
K mg/g	0.25(*)	-0.44**	NS	NS	-0.32*	NS
Mg mg/g	0.38**	NS	NS	0.28*	NS	0.31*
Mo ug/g	NS	NS	NS	NS	NS	NS
Mn ug/g	NS	NS	NS	NS	NS	NS
Na ug/g	-0.40**	NS	NS	NS	NS	NS
P ug/g	NS	NS	NS	NS	-0.36*	NS
CEC	NS	NS	NS	NS	NS	-0.32*
BS	NS	-0.37**	NS	NS	-0.39*	NS
pH (CaCl2)	NS	NS	NS	NS	NS	NS

(*) ($p < 0.1$)
* ($p < 0.05$)
** ($p < 0.01$)
*** ($p < 0.001$)

Table 2B Spearman correlations for Microbial N and C, Dissolved Organic Nitrogen (DON) and Mg (mg/g) and the soil chemistry parameters measured via ICP. CEC = cation Exchange Capacity, BS = Base Saturation. All figures were measured at a soil depth of 10 – 30cm

	Microbial N	Microbial C	DON	Mg (mg/g)	pH (CaCl2)
Al ug/g	NS	NS	NS	NS	-0.33*
Ca mg/g	NS	NS	NS	0.46***	NS
Cd ug/g	NS	NS	-0.25 (*)	NS	NS
Cu ug/g	NS	NS	NS	NS	NS
Hg ug/g	NS	NS	NS	0.90***	NS
K mg/g	NS	NS	NS	NS	NS
Mg mg/g	NS	NS	NS		NS
Mo ug/g	NS	NS	NS	-0.32*	NS
Mn ug/g	NS	NS	NS	NS	-0.57***
Na ug/g	NS	NS	NS	NS	NS
P ug/g	NS	NS	0.37**	NS	-0.44**
CEC	NS	NS	NS	NS	NS
BS	NS	NS	NS	NS	NS
pH (CaCl2)	NS	NS	NS	NS	

(*) ($p < 0.1$)
* ($p < 0.05$)
** ($p < 0.01$)
*** ($p < 0.001$)

Table 3 Spearman correlations between vitality, vital root mass, n root tips, mycorrhizal colonization, in-growth bag mycelia, n EcM morphotypes, microbial N and microbial C from Viennese street tree planting pits. All figures were measured at a soil depth of 10 – 30cm

	Vitality	Root Biomass	Root tips	EcM Col.	Mycelia	Morphotypes	Microbial N	Microbial C	DON
Vitality	1								
Root Biomass	NS	1							
Root Tips	NS	0.59***	1						
EcM Col.	NS	NS	NS	1					
Mycelia	-0.33*	NS	NS	NS	1				
Morphotypes	NS	0.30*	0.28*	NS	NS	1			
Microbial N	NS	NS	NS	NS	0.48**	NS	1		
Microbial C	NS	NS	NS	NS	NS	NS	0.46***	1	
DON	NS	NS	NS	NS	-0.39*	NS	NS	NS	1

Table 4 Spearman correlations between the percentage of the four major cations occupied by each cation in soils. **Na%** is the percentage of Na + Ca + Mg + K occupied by Na, **Ca%** the percentage occupied by Ca, **Mg%** the percentage occupied by Mg, and **K%** the percentage occupied by K. Letters denote p values close to α=0.05

Correlation	All	Park	Side	Main
Na% - Ca%	-0.27(*)	NS	-0.50*	-0.83***
Na % - Mg%	NS	NS	0.42(*)	0.52(*)
Na% - K%	NS	NS	NS	0.57*
Ca% - Mg%	-0.64***	-0.82***	-0.57*	-0.74**
Ca% - K%	-0.55***	-0.74***	NS	-0.70**
Mg% - K%	NS	NS	NS	NS

(*) ($p < 0.1$)
* ($p < 0.05$)
** ($p < 0.01$)
*** ($p < 0.001$)

Table 5 Spearman correlations between the percentages of the four major cations occupied by each cation in soils and vitality and mycorrhizal parameters. EcM col. = proportion of root tips colonised by mycorrhiza. Mycelia = mycelial presence and intensity in mesh bags. Morphotypes = number of morphotypes per sample. Vitality = tree vitality score according to Vienna municipality criteria. Letters denote p values close to α=0.05

	EcM Col.	Mycelia	Morphotypes	Vitality
Na%	NS	NS	-0.26 (*)	-0.37**
Ca%	NS	0.31 (*)	NS	NS
Mg%	0.38**	-0.37*	0.34*	0.39**
K%	NS	-0.27 (*)	NS	NS

(*) ($p < 0.1$)
* ($p < 0.05$)
** ($p < 0.01$)
*** ($p < 0.001$)

Table 6 Spearman correlations between soil cation ratios and vitality and mycorrhizal parameters. Ratios are calculated from the mass of elements (mg/g). EcM col. Is the proportion of root tips colonised by mycorrhiza. Mycelia = mycelial presence and intensity in mesh bags. Morphotypes = number of morphotypes per sample. Vitality = tree vitality score according to Vienna municipality criteria. Root tips = number of root tips per sample in 10 -30cm core depth

	Vitality	Root tips	Root Biomass	EcM Col.	Mycelia	Morphotypes
Ca:Na	0.42**	NS	NS	0.36**	NS	NS
Ca:Mg	-0.37*	-0.32*	NS	-0.31*	0.40*	NS
Ca:K	NS	NS	0.32*	NS	0.31*	NS
Ca:P	NS	NS	NS	NS	0.33*	NS
K:Na	0.48***	NS	NS	0.36**	-0.34*	NS
Mg : K	NS	0.26 (*)	0.36*	0.29*	NS	0.31
Mg:Na	0.57***	NS	NS	0.44**	-0.40*	0.31*
P:Na	0.37**	NS	NS	NS	-0.39*	0.31*
P:Mg	NS	NS	NS	NS	NS	NS
P:K	NS	NS	NS	NS	NS	NS

(*) ($p < 0.1$)
* ($p < 0.05$)
** ($p < 0.01$)
*** ($p < 0.001$)

Discussion

Numerous studies have shown that vitality of urban roadside trees is compromised by urban stresses (Czerniawska-Kusza et al. 2004, Gauszka et al. 2011, Sand et al. 2018). Aboveground vitality scores of *Tilia sp.* trees declined with increasing intensity of urban stress, confirming that this was also the case for the trees in this study (Figure 6A). Trees in main streets showed the lowest vitality, whereas park trees showed the highest vitality. Root biomass, however, tended to be lower in parks than either street location, with no significant differences between locations (Figure 7A). Root biomass undergoes seasonal changes, and has been shown to peak in *Tilia sp.* in early summer or at a temperature of around 20°C (Meinen et al. 2009). Our root samples were collected in July just after this peak period. There was no correlation found between vitality and root biomass (Table 3), indicating that root biomass is not a suitable positive indicator of the above ground health of the trees in this study. Under drought stress conditions such as that found in urban environments, *Tilia sp*. have been known to decrease in root investment in upper soil layers and increase investment in deeper layers (Stratópoulos et al. 2019). We found a trend towards increased root biomass in locations with increased intensity of urban stresses in the 30 – 50 cm soil depth (Figure 7D), and we measured greatest root biomass in side street trees at 10 – 30cm soil depth (Figure 7C). This is also reflected in a higher root density in side streets (Figure 7I). Roadside trees often endure restricted space for root growth (Bühler et al. 2017), and this may lead to this greater root density in these planting pits. The exposure to urban stress therefore not only resulted in lower vitality in the street trees in our study, but also resulted in differences in rooting behaviour.

We hypothesised that sodium from de-icing salts plays a role in the loss of vitality in urban trees. Exchangeable soil Na^+ (µg/g) was negatively correlated with aboveground vitality (Table 2A), as was exchangeable Na% (Table 5). This relationship was influenced by location: the lowest sodium levels were in park soils and highest in main streets, which was the opposite pattern to vitality (Figure 8A, 10C). This was also reflected in the ratios of the other base cations to Na^+ (Figure 11). The application of de-icing salt is responsible for the differences in extractable sodium levels found between locations in this study. This is in agreement with other studies, which found that soil sodium levels decreased with greater distance from roads where de-icing salts were applied (Bryson and Barker 2002, Cekstere and Osvalde 2013). The lack of difference in extractable Na^+ between main street and side street soils may be explained by the application of de-icing salts on footpaths in side streets, which enter the soil via runoff, as there are usually no kerbs to protect the trees from this input. While the street soils had mean Na^+ levels that were over double that of the parks (Figure 8A), most soils had Na^+ levels that were under the threshold of 250 µg/g that is considered too high for most tree species (Hootman et al. 1994). However, we sampled soils in October, and the Na^+ (µg/g) levels measured were probably lower at this time than

earlier in the year due to a washing out of sodium over the course of the vegetation period (Asensio et al. 2017). It is therefore likely that sodium negatively affecting the vitality of the trees in this study is present in much higher levels in the soil for much of the year. Tree vitality can be negatively affected by salt in numerous ways (Paludan-Müller et al. 2002, Gałuszka et al. 2011). High levels of sodium chloride can result in drought stress in trees due to high osmotic pressure (Kayama et al. 2003). High Na^+ and Cl^- concentrations in soils can lead to increased uptake of these ions into the plant material, occurring often with a simultaneous reduction in uptake of base cations such as Ca^{2+} and K^+ resulting in nutrient imbalances in the leaves (Kayama et al. 2003, Czerniawska-Kusza et al. 2004, Dmuchowski et al. 2014). Although these parameters were not measured in our study, it is highly likely that they contribute to the lower vitality of trees in the street locations. Salt application can cause nutrient imbalances to occur not only in plant tissue but also in soils (Bryson and Barker 2002). The vitality of the trees in this study was positively correlated with Ca : Na, K : Na, Mg : Na and P : Na ratios (Table 6) which were all highest in parks (Figure 11), further indicating that trees were healthier where sodium levels were lower.

However, high levels of calcium can also be problematic for urban vegetation (Craul 1985, Kleiber et al. 2019). Our soils had high amounts of exchangeable calcium (Figure 9A), which constituted on average over 90% of the exchangeable base cations in all locations (Figure 10A). Numerous studies have shown that urban soils have high levels of exchangeable Ca^{2+}, despite a diversity of parent material (Bain et al. 2012, Wu et al. 2018), partly due to weathering of calcium rich building materials such as cement and concrete (Kaushal et al. 2014, Washbourne et al. 2015, Chambers et al. 2016). This high calcium content led to a cation exchange capacity of between 268 and 366 µmol/g (figure 8B), and base saturations of 99.5% to 99.8%, both of which can be characterised as very high (Leitgeb 2013). All locations in our study had similar mean levels of exchangeable Ca^{2+} (Figure 9A) which ranged from 4.95 to 6.99 mg/g. These ranges were comparable to exchangeable calcium levels in urban soils in other cities (Cekstere and Osvalde 2013, Li et al. 2013, Karliński et al. 2014), and below the exchangeable calcium levels measured on urban soils in Vienna by Simon et al. (2013). Despite the high Ca^{2+} levels found during soil analysis, neither soil Ca^{2+} (mg/g) (Table 2A) nor did exchangeable Ca% (Table 5) correlated negatively to aboveground vitality. There was also no correlation between pH levels and Ca^{2+} or vitality of the trees in our study (Table 2A), despite pH levels in urban soils being known to increase because of high calcium levels from building materials (Greinert 2015). PH levels measured in our soils ranged from 6.1 to 7.4 in $CaCl_2$; corresponding to a range of slightly acidic to slightly alkaline (Leitgeb 2013), and these values were similar to other studies on urban vegetation (Czerniawska-Kusza et al. 2004, Cekstere and Osvalde 2013, Kleiber et al. 2019). The elevated soil calcium levels in our soils did not correlate to soil pH, and we cannot directly attribute Ca^{2+} or pH levels directly to loss of vitality in the *Tilia sp*. we examined.

Elevated soil calcium and sodium levels may cause indirect problems for urban trees such as leaching of other base cations from exchange sites leading to soil nutrient imbalances (Craul 1985). Expressing each soil base cation as a percentage of the total amount of soil base cations (Na%, Ca%, Mg%, K% - see equations 6 -9) allows us to compare the share of base saturation occupied by exchangeable Na^{+}, Ca^{2+}, Mg^{2+}, or K^{+}, and to assess how the proportion of each cation relates to each other. Contrary to our hypothesis that Na+ would lead to nutrient imbalances in the soil, all base cation percentages were negatively correlated with Ca% (Table 4). High Ca^{2+} levels in urban soils can be antagonistic to the other base cations on exchange sites, resulting in leaching of these nutrients (Craul 1985, Pröll et al. 2015). We broke down the correlations of the cation percentages into the different locations to determine how increased Na^{+} input in streets affects the other base cations (Table 4). Most correlations were found in main street soils, where sodium was highest and tree vitality was lowest. We found exchangeable K% was positively correlated to Na% in main street soils. This could be due to exchangeable soil Na+ ions replacing "fixed" K+ ions from between layers of clay minerals and forcing these cations into the "exchangeable" K+ pool (Norrström and Bergstedt 2001). Mg% decreased with increasing urban stress (Figure 10D) and was positively correlated with vitality, EcM morphotypes and colonization rates (Table 5) which suggest it is a common factor in both above ground and below ground health of urban trees (Musio et al. 2007). A negative correlation between Ca% and Mg% was found across all soil groups (Table 4), and as Ca^{2+} levels were fairly constant in all locations it is possible that the lower Mg^{2+} levels in main streets (Figure 9C) is due to lower Mg^{2+} inputs in these soils. This may be due to a removal of Mg^{2+} from nutrient cycles when leaf litter is removed from the area around street trees in autumn. The correlation between Mg^{2+} and Hg^{2+} (Table 2B) indicates this possibility, as both Mg^{2+} and Hg^{2+} is known to enter nutrient cycles through leaf tissue, and circulate between leaves and soil via uptake by tree roots (Demers et al. 2007, Langenbruch et al. 2012, Gregory van der et al. 2014). Nutrient ratios also point to magnesium as a limiting nutrient in our soils (Figure 12). The soil Ca : Mg ratio has an optimum for tree health of between 6:1 and 8 : 1 (Cekstere and Osvalde 2013, Kleiber et al. 2019). This was greatly exceeded in our soils: the lowest levels were in parks at 22:1 (Figure 12A). This was confirmed in our results by the negative correlation between the Ca : Mg and vitality, EcM colonization and with the number of root tips. Another important ratio is the soil Mg : K ratio, which has optimal levels at 2:1 (Cekstere and Osvalde 2013). The soil Mg : K ratios in our study were lower, ranging from 0.39 to 1.86, however this was not reflected in a relationship between the Mg : K ratio and above ground vitality (Table 6). The magnesium levels in the street soils were around 0.2 mg/g, which corresponds to a medium level in the context of forest soils (Leitgeb 2013). Nonetheless, soil exchangeable magnesium is the cation that appears to play a central role in the vitality of street trees, as it is positively correlated to numerous parameters. Repeated measurements of soil Mg^{2+} levels could determine if Mg^{2+} is being lost from these urban soils in the long term.

Cadmium is a heavy metal that enters the soils in urban areas through industrial and traffic emissions

and can be detrimental to plant health and development (Benavides et al. 2005, Lee et al. 2005). This was apparent in our results in the negative correlation between Cadmium and tree vitality (Table 2). Despite the negative correlation with vitality, the cadmium levels in our soils ranged from 0.0033 µg/g to 0.05 µg/g (Figure 14B): well below contaminated levels (Alagić et al. 2013, Kleiber et al. 2019). Cadmium levels had a trend that increased with increasing urban conditions (Figure 14B), and higher cadmium levels occurred in main streets where other urban stress factors also occurred, which may also partially explain the negative correlation between cadmium and vitality. Copper is a heavy metal that is known to be toxic to fungi, and is often a component of vineyard fungicides (Wightwick et al. 2008). Copper enters urban soils through the deposition of particulates from brake and tire wear (Sturtz et al. 2014). Although copper levels were similar in all locations (figure 14A), it was negatively correlated with both root biomass and with number of EcM morphotypes. Tilia are not known to be susceptible to copper contamination, and can tolerate levels of copper much higher than those found in our soils without showing negative symptoms (Serbula et al. 2013). It is possible that the fungicidal properties of copper are reflected in the negative correlation with the number of EcM morphotypes. Fungal biomass has a higher C:N ratio than bacterial biomass, and the C:N ratio of microbial biomass can therefore offer an insight into microbial community structure (Zhou et al. 2019). The microbial C:N ratio was around 10 in all locations (Figure 16 C) and was not correlated with copper or any other parameter, indicating that copper levels in our soils did not negatively impact the fungal community. Although both copper and cadmium are known to have negative effects on urban trees and fungi, there was no evidence in our data to suggest that copper plays a major role in the loss of vitality in our trees. The negative relationship between cadmium and vitality indicate that Cd^{2+} contributes to a cumulative negative effect caused by numerous urban stress factors on the health of the trees in our study.

Studies have shown that mycorrhiza can improve the health of trees where nutrient imbalances and salt stress are factors (Zwiazek et al. 2019). The percentage of fine roots colonized by mycorrhiza was greatest in parks and decreased with increasing urban stress - the opposite pattern to soil sodium (Figure 10A) although there was no correlation (Table 2A). Furthermore, despite having a similar pattern according to location, EcM colonization and vitality were not positively correlated (Table 3). Therefore we could not find direct evidence that there was a positive relationship between EcM colonization and the vitality of the trees in this study. However, EcM colonization percentage was positively correlated with soil exchangeable magnesium which was positively correlated with tree vitality (Table 2A). Soil exchangeable Na% (Table 5) was also not correlated to EcM colonization despite a negative correlation with vitality. However, EcM colonization was positively correlated with soil Ca : Na, Mg : Na, and K : Na ratios (Table 6), which suggests that colonisation was more abundant where exchangeable Na^{+} was proportionally lower than other base cations. Sodium also had no relationship with number of morphotypes or with in-growth bag mycelia, the latter correlating negatively with tree vitality. Not only does sodium wash out of soils over the year, but mycorrhizal

colonisation can fluctuate due to seasonal changes (Swaty et al. 1998), and there was a three month period between sampling for mycorrhizal colonization and morphotypes and our soil chemical analysis. The relationship between sodium and both ectomycorrhizal colonisation and number of morphotypes could therefore be underestimated in our analysis. Sampling of both soil and mycorrhizae at intervals over the vegetation period could better determine how mycorrhizae react to soil sodium levels in urban *Tilia sp.*

Fragmentation effects due to isolated street tree planting pits and strips are thought to prevent street trees from colonization by potentially beneficial mycorrhizae species that can withstand the greater urban stress in these locations (Tyburska et al. 2013). The diversity of ectomycorrhizal morphotypes on *Tilia sp.* has been shown to be lower for street trees than forest trees (Nielsen and Rasmussen 1999). In our study, we used park trees rather than forest trees for our control but we still expected a higher amount of diversity due to decreased urban stress and lower fragmentation effects in the park sites. However, we found no significant differences between locations for the number of ectomycorrhizal morphotypes per sample: each had on average of 2 – 4 morphotypes. This was lower than previous studies on urban *Tilia* trees (Nielsen and Rasmussen 1999, Timonen and Kauppinen 2008). Simpson diversity scores for morphotypes were highest in the parks and lowest in the side streets, but indices for each treatment were similarly high: between 0.844 and 0.874 suggesting that morphotype diversity is not dependant on the level of urban stress. Across all samples, the number of mycorrhizal morphotypes per tree tended to be higher where the number of root tips were greater and where magnesium levels were higher (Table 3). As stated above, exchangeable soil magnesium was higher in parks (Figure 8C), possibly due to inputs into the park soils from decomposing leaf litter (Langenbruch et al. 2012). Organic matter can help keep soil loose and more aerated, which can result in greater abundance of root tips and more stimulated root growth (Karliński et al. 2014). EcM morphotypes had a positive correlation to root biomass. More abundant root growth may simply create more habitats for mycorrhizae in these soils. Although we did not find differences in morphotype diversity between locations, numerous ectomycorrhizal species can have similar morphotypes that are hard to differentiate (Timonen and Kauppinen 2008), so the diversity at a species level may differ to the findings at morphological level. DNA analysis could provide a clearer picture of EcM diversity in these soils.

Ectomycorrhizae are known to engage in long-distance foraging strategies where soils are poorer (Jílková et al. 2017). Mycelia are formed during long-range exploration by mycorrhizae, and can obtain carbon from their host thereby exploring substrates with little or no organic matter, such as those contained in the mesh bags (Wallander et al. 2001). Mycelia harvested in mesh ingrowth bags were generally more abundant where conditions were less favourable for the host trees, and this was reflected in a negative correlation between in-growth bag mycelia and vitality (Table 3). In parks, mycelia were found in only about 30% of harvested ingrowth bags, whereas around 80% of

harvested ingrowth bags from side streets and 90% of those in main streets were found to have mycelia, and this pattern was similar for rhizomorphs. Mycelia in our study correlated negatively to extractable soil P (µg/g), but also to extractable soil K (mg/g) (Table 2A). Plants are known to invest in mycorrhizae where soils are P deficient (Wallander and Thelin 2008) to allow foraging for nutrient hotspots (Chen et al. 2018). Mycelia also had a negative relationship with Dissolved Organic Nitrogen (DON) (Table 3). DON was lower in main streets than the other locations (Figure 13A). DON is often inputted into soils by leaf litter (Uselman et al. 2012), and much like with Mg^{2+} leaf litter removal could be a reason for the lower levels of DON on main streets. DON can also enter soil through animal excrement (Gonet and Debska 2006), and it is possible that the higher levels of DON in side streets are due to inputs from domestic dogs as these streets were often in residential areas. The extramatrical mycelia has been shown to be less abundant where nitrogen is higher (Arnebrant 1994). Greater availability of soil N and nutrients favours ectomycorrhizae that tend to employ short-range exploration strategies rather than long distance strategies (Hobbie and Agerer 2010, Defrenne et al. 2019). In general, the correlations between biological parameters and both nutrient ratios (Table 6) and cation percentages (Table 5) indicate that where Ca^{2+} and Na^{+} are higher and Mg^{2+} is lower, the trees in our study tend to be less vital, have lower EcM root tip colonization, and tend to be colonized more by mycorrhizae that employ long distance foraging strategies. This possibly reflects a reduction in photosynthetic sugars allocated to mycorrhizae when the vitality of trees is reduced. Improving the nutrient balance in street soils, especially to improve levels of Mg^{2+}, P^{+}, K^{+} and DON could therefore be beneficial to street trees and their symbionts and should be considered in measures aimed at improving the health and longevity of urban trees.

Conclusion

Urban trees must endure many simultaneous stress factors such as drought conditions, soil compaction, salt application, nutrient imbalances, soil contamination, and high temperatures in order to deliver the valuable ecosystem services they provide (Pauleit et al. 2002). What is clear from our data is that street trees that are more exposed to these stresses are not as healthy as those in parks that are growing in conditions that are more favourable. We hypothesised that the differences in health were due to salt application, and as such expected to find correlations between sodium and biological parameters. We found that although sodium levels did correlate negatively with vitality, this was part of a wider nutrient imbalance caused on the one hand by high Ca^{2+} levels and on the other hand by receding magnesium levels in the street soils. This imbalance not only coincided with differences in tree health, but also differences in mycorrhizal behaviour. Cadmium from traffic emissions also had a negative effect on tree vitality, and this should not be discounted as an urban stress factor.

The levels of soil sodium may be somewhat underestimated in our study, due to soil sampling occurring quite late in the year. It is likely that sodium levels in mid-summer are higher than in autumn, combining drought stress from the high temperatures in summer with osmotic stress from sodium. It is also likely that sodium levels differ from year to year depending on the amount of snowfall occurring the previous winter. To fully understand the patterns of sodium in street soils and its effect on the trees in our study, it is our opinion that a sampling of both soils and leaves at regular intervals over the course of a vegetation period would be useful. This would also provide a direct measure of the sodium and chloride uptake by the trees, and could quantify leaching effects. Nevertheless, it is clear from our data that the application of de-icing salt is detrimental to the health of street trees and plays a major part in the nutrient imbalance found in our soils.

Magnesium was associated with many biological parameters in our study; it had positive relationships with tree vitality and with mycorrhizal parameters such as colonization percentage and morphotype diversity, and was negatively correlated to in-growth bag mycelia that were more abundant in poorer soils. It is fair to say that where Mg^{2+} levels were higher, trees were healthier, had greater levels of EcM colonization by contact exploration types, and had a greater EcM morphotype diversity. Lower Mg^{2+} and DON levels in main streets could be a result of leaf litter removal resulting in poorer soils in these locations. Allowing leaf litter to decompose in the direct vicinity of street trees could be a cost effective way to improve the health of these valuable trees and their symbionts, and reduce nutrient imbalances in urban soils.

References

Alagić, S. Č., S. S. Šerbula, S. B. Tošić, A. N. Pavlović, and J. V. Petrović. 2013. Bioaccumulation of Arsenic and Cadmium in Birch and Lime from the Bor Region. Archives of Environmental Contamination and Toxicology **65**:671-682.

Arantes, B. L., T. Mauad, and D. F. D. S. Filho. 2019. Urban Forests, Air Quality and Health: A Systematic Review. International Forestry Review **21**:167-181, 115.

Arnebrant, K. 1994. Nitrogen amendments reduce the growth of extramatrical ectomycorrhizal mycelium. Mycorrhiza **5**:7-15.

Asensio, E., V. J. Ferreira, G. Gil, T. García-Armingol, A. M. López-Sabirón, and G. Ferreira. 2017. Accumulation of De-Icing Salt and Leaching in Spanish Soils Surrounding Roadways. International journal of environmental research and public health **14**:1498.

Bäckström, M., S. Karlsson, L. Bäckman, L. Folkeson, and B. Lind. 2004. Mobilisation of heavy metals by deicing salts in a roadside environment. Water Research **38**:720-732.

Bain, D. J., I. D. Yesilonis, and R. V. Pouyat. 2012. Metal concentrations in urban riparian sediments along an urbanization gradient. Biogeochemistry **107**:67-79.

Benavides, M. P., S. M. Gallego, and M. L. Tomaro. 2005. Cadmium toxicity in plants. Brazilian Journal of Plant Physiology **17**:21-34.

Bryson, G. M., and A. V. Barker. 2002. Sodium accumulation in soils and plants along Massachusetts roadsides. Communications in Soil Science and Plant Analysis **33**:67-78.

Bühler, O., M. Ingerslev, S. Skov, E. Schou, I. M. Thomsen, C. N. Nielsen, and P. Kristoffersen. 2017. Tree development in structural soil – an empirical below-ground in-situ study of urban trees in Copenhagen, Denmark. Plant and Soil **413**:29-44.

Cekstere, G., and A. Osvalde. 2013. A study of chemical characteristics of soil in relation to street trees status in Riga (Latvia). Urban Forestry & Urban Greening **12**:69-78.

Chambers, L. G., Y.-P. Chin, G. M. Filippelli, C. B. Gardner, E. M. Herndon, D. T. Long, W. B. Lyons, G. L. Macpherson, S. P. McElmurry, C. E. McLean, J. Moore, R. P. Moyer, K. Neumann, C. A. Nezat, K. Soderberg, N. Teutsch, and E. Widom. 2016. Developing the scientific framework for urban geochemistry. Applied Geochemistry **67**:1-20.

Chen, W., R. T. Koide, and D. M. Eissenstat. 2018. Nutrient foraging by mycorrhizas: From species functional traits to ecosystem processes. Functional Ecology **32**:858-869.

Craul, P. J. 1985. A description of urban soils and their desired characteristics. Journal of Arboriculture **11**:330-339.

Cunningham, M. A., E. Snyder, D. Yonkin, M. Ross, and T. Elsen. 2008. Accumulation of deicing salts in soils in an urban environment. Urban Ecosystems **11**:17-31.

Czerniawska-Kusza, I., G. Kusza, and M. Dużyński. 2004. Effect of deicing salts on urban soils and health status of roadside trees in the Opole region. Environmental Toxicology **19**:296-301.

Defrenne, C. E., T. J. Philpott, S. H. A. Guichon, W. J. Roach, B. J. Pickles, and S. W. Simard. 2019. Shifts in Ectomycorrhizal Fungal Communities and Exploration Types Relate to the Environment and Fine-Root Traits Across Interior Douglas-Fir Forests of Western Canada. Frontiers in Plant Science **10**.

Demers, J. D., C. T. Driscoll, T. J. Fahey, and J. B. Yavitt. 2007. Mercury Cycling in Litter and Soil in Different Forest Types in the Adirondack Region, New York, USA. Ecological Applications **17**:1341-1351.

Dixon, R. K., M. V. Rao, and V. K. Garg. 1993. Salt stress affects in vitro growth and in situ symbioses of ectomycorrhizal fungi. Mycorrhiza **3**:63-68.

Dmuchowski, W., B. Rutkowska, W. Szulc, and A. Baczewska. 2014. Effect of salt stress caused by deicing on the content of microelements in leaves of linden. Journal of Elementology.

Dresden, T. 2015. Citree - Woody species for urban spaces.

Gałuszka, A., Z. M. Migaszewski, R. Podlaski, S. Dołęgowska, and A. Michalik. 2011. The influence of chloride deicers on mineral nutrition and the health status of roadside trees in the city of Kielce, Poland. Environmental Monitoring and Assessment **176**:451-464.

Gauszka, A., Z. M. Migaszewski, R. Podlaski, S. Dogowska, and A. Michalik. 2011. The influence of chloride deicers on mineral nutrition and the health status of roadside trees in the city of Kielce, Poland. Environmental Monitoring and Assessment **176**:451-464.

German, D. P., M. N. Weintraub, A. S. Grandy, C. L. Lauber, Z. L. Rinkes, and S. D. Allison. 2011. Optimization of hydrolytic and oxidative enzyme methods for ecosystem studies. Soil Biology and Biochemistry **43**:1387-1397.

Gonet, S. S., and B. Debska. 2006. Dissolved organic carbon and dissolved nitrogen in soil under different fertilization treatments. Plant, Soil and Environment **52**:55-63.

Gregory van der, H., A. Legout, B. Pollier, J. Ranger, and E. Dambrine. 2014. The dynamics of calcium and magnesium inputs by throughfall in a forest ecosystem on base poor soil are very slow and conservative: evidence from an isotopic tracing experiment (^{26}Mg and ^{44}Ca). Biogeochemistry **118**:413-442.

Greinert, A. 2015. The heterogeneity of urban soils in the light of their properties. Journal of Soils and Sediments **15**:1725-1737.

Hobbie, E., and R. Agerer. 2010. Nitrogen isotopes in ectomycorrhizal mushrooms correspond to belowground exploration types.

Hootman, R. G., P. D. Kelsey, R. Reid, and K. Von Der Heide-Spravka. 1994. Factors affecting accumulation of deicing salts in soils around trees. Journal of arboriculture. **20**:196-201.

Jenkinson, D. S., and D. S. Powlson. 1976. The effects of biocidal treatments on metabolism in soil—V: A method for measuring soil biomass. Soil Biology and Biochemistry **8**:209-213.

Jílková, V., M. Vohník, J. Dauber, A. Marten, H. Šimáčková, and J. Frouz. 2017. Low root biomass and occurrence of ectomycorrhizal exploration types in inhabited wood ant (Formica polyctena) nests in a temperate spruce forest. European Journal of Soil Biology **79**:57-62.

Jim, C. Y., and W. Y. Chen. 2008. Assessing the ecosystem service of air pollutant removal by urban trees in Guangzhou (China). Journal of Environmental Management **88**:665-676.

Joergensen, R. G. 1996. The fumigation-extraction method to estimate soil microbial biomass: Calibration of the kEC value. Soil Biology and Biochemistry **28**:25-31.

Joergensen, R. G., and T. Mueller. 1996. The fumigation-extraction method to estimate soil microbial biomass: Calibration of the kEN value. Soil Biology and Biochemistry **28**:33-37.

Karliński, L., A. M. Jagodziński, T. Leski, P. Butkiewicz, M. Brosz, and M. Rudawska. 2014. Fine root parameters and mycorrhizal colonization of horse chestnut trees (Aesculus hippocastanum L.) in urban and rural environments. Landscape and Urban Planning **127**:154-163.

Kaushal, S. S., W. H. McDowell, and W. M. Wollheim. 2014. Tracking evolution of urban biogeochemical cycles: past, present, and future. Biogeochemistry **121**:1-21.

Kayama, M., A. M. Quoreshi, S. Kitaoka, Y. Kitahashi, Y. Sakamoto, Y. Maruyama, M. Kitao, and T. Koike. 2003. Effects of deicing salt on the vitality and health of two spruce species, Picea abies Karst., and Picea glehnii Masters planted along roadsides in northern Japan. Environmental Pollution **124**:127-137.

Kleiber, T., M. Krzyżaniak, D. Świerk, A. Haenel, and S. Gałecka. 2019. How does the content of nutrients in soil affect the health status of trees in city parks? PLOS ONE **14**:e0221514.

Kuttler, W. 2011. Climate change in urban areas, Part 1, Effects. Environmental Sciences Europe **23**:11.

Lang, C., J. Seven, and A. Polle. 2011. Host preferences and differential contributions of deciduous tree species shape mycorrhizal species richness in a mixed Central European forest. Mycorrhiza **21**:297-308.

Langenbruch, C., M. Helfrich, and H. Flessa. 2012. Effects of beech (Fagus sylvatica), ash (Fraxinus excelsior) and lime (Tilia spec.) on soil chemical properties in a mixed deciduous forest. Plant and Soil **352**:389-403.

Lee, P.-K., Y.-H. Yu, S.-T. Yun, and B. Mayer. 2005. Metal contamination and solid phase partitioning of metals in urban roadside sediments. Chemosphere **60**:672-689.

Lehto, T., and J. J. Zwiazek. 2011. Ectomycorrhizas and water relations of trees: a review. Mycorrhiza **21**:71-90.

Leitgeb, E., Reiter R., Englisch, M.,Lüscher, P., Schad, P., Feger, K. 2013. Waldböden: Ein Bildatlas der wichtigsten Bodentypen aus Österreich, Deutschland und der Schweiz. Pages 13-53. Wiley-VCH Verlag & Co KGaA, Weinheim, Germany.

Li, Z.-g., G.-s. Zhang, Y. Liu, K.-y. Wan, R.-h. Zhang, and F. Chen. 2013. Soil Nutrient Assessment for Urban Ecosystems in Hubei, China. PLOS ONE **8**:e75856.

Meinen, C., D. Hertel, and C. Leuschner. 2009. Root Growth and Recovery in Temperate Broad-Leaved Forest Stands Differing in Tree Species Diversity. Ecosystems **12**:1103-1116.

Musio, M., M. Musio, K. von Wilpert, K. von Wilpert, N. H. Augustin, and N. H. Augustin. 2007. Crown condition as a function of soil, site and tree characteristics. European Journal of Forest Research **126**:91-100.

Newbound, M., M. A. McCarthy, and T. Lebel. 2010. Fungi and the urban environment: A review. Landscape and Urban Planning **96**:138-145.

Nielsen, J. S., and H. N. Rasmussen. 1999. MYCORRHIZAL STATUS AND MORPHOTYPE DIVERSITY IN TILIA CORDATA - A PILOT STUDY OF NURSERIES AND URBAN HABITATS. Pages 451-460. International Society for Horticultural Science (ISHS), Leuven, Belgium.

Norrström, A. c., and E. Bergstedt. 2001. The Impact of Road De-Icing Salts (NaCl) on Colloid Dispersion and Base Cation Pools in Roadside Soils. Water, Air and Soil Pollution **127**:281-299.

Nowak, D. J., S. Hirabayashi, A. Bodine, and R. Hoehn. 2013. Modeled PM2.5 removal by trees in ten U.S. cities and associated health effects. Environmental Pollution **178**:395-402.

Paludan-Müller, G., H. Saxe, L. B. Pedersen, and T. B. Randrup. 2002. Differences in salt sensitivity of four deciduous tree species to soil or airborne salt. Physiologia Plantarum **114**:223-230.

Pauleit, S., N. Jones, G. Garcia-Martin, J. L. Garcia-Valdecantos, L. M. Rivière, L. Vidal-Beaudet, M. Bodson, and T. B. Randrup. 2002. Tree establishment practice in towns and cities – Results from a European survey. Urban Forestry & Urban Greening **1**:83-96.

Pröll, G., P. Hietz, C. M. Delaney, and K. Katzensteiner. 2015. Substrate influences ecophysiological performance of tree seedlings. Tree Physiology **36**:39-53.

Rewald, B., L. Holzer, and H. Göransson. 2015. Arbuscular mycorrhiza inoculum reduces root respiration and improves biomass accumulation of salt-stressed Ulmus glabra seedlings. Urban Forestry & Urban Greening **14**:432-437.

Sand, E., J. Konarska, A. W. Howe, Y. Andersson-Sköld, F. Moldan, H. Pleijel, and J. Uddling. 2018. Effects of ground surface permeability on the growth of urban linden trees. Urban Ecosystems **21**:691-696.

Schiop, S. T., M. Al Hassan, A. F. Sestras, M. Boscaiu, R. E. Sestras, and O. Vicente. 2015. Identification of salt stress biomarkers in Romanian Carpathian populations of Picea abies (L.) Karst. PLoS ONE **10**:e0135419.

Serbula, S. M., T. S. Kalinovic, A. A. Ilic, J. V. Kalinovic, and M. M. Steharnik. 2013. Assessment of Airborne Heavy Metal Pollution Using Pinus spp. and Tilia spp. Aerosol and Air Quality Research **13**:563-573.

Stratópoulos, L. M. F., C. Zhang, S. Duthweiler, K.-H. Häberle, T. Rötzer, C. Xu, and S. Pauleit. 2019. Tree species from two contrasting habitats for use in harsh urban environments respond differently to extreme drought. International Journal of Biometeorology **63**:197-208.

Sturtz, T. M., S. D. Adar, T. Gould, and T. V. Larson. 2014. Constrained source apportionment of coarse particulate matter and selected trace elements in three cities from the multi-ethnic study of atherosclerosis. Atmospheric Environment **84**:65-77.

Sucoff, E. 1975. Deicing salt (sodium chloride) damage to Pinus resinosa Ait. Canadian journal of forest research = **v. 5**:pp. 546-556-1975 v.1975 no.1974.

Swaty, R. L., C. A. Gehring, M. Van Ert, T. C. Theimer, P. Keim, and T. G. Whitham. 1998. Temporal variation in temperature and rainfall differentially affects ectomycorrhizal colonization at two contrasting sites. New Phytologist **139**:733-739.

Taha, H. 1997. Urban climates and heat islands: albedo, evapotranspiration, and anthropogenic heat. Energy and Buildings **25**:99-103.

Taylor, M. S., B. W. Wheeler, M. P. White, T. Economou, and N. J. Osborne. 2015. Research note: Urban street tree density and antidepressant prescription rates—A cross-sectional study in London, UK. Landscape and Urban Planning **136**:174-179.

Timonen, S., and P. Kauppinen. 2008. Mycorrhizal colonisation patterns of Tilia trees in street, nursery and forest habitats in southern Finland. Urban Forestry & Urban Greening **7**:265-276.
Tyburska, J., A. Frymark-Szymkowiak, M. Kulczyk-Skrzeszewska, and B. Kieliszewska-Rokicka. 2013. Mycorrhizal status of forest trees grown in urban and rural environments in Poland. Ecological Questions **18**:49-57.
Urban, J. 2008. Up by roots: healthy soils and trees in the built environment.
Uselman, S. M., R. G. Qualls, and J. Lilienfein. 2012. Quality of soluble organic C, N, and P produced by different types and species of litter: Root litter versus leaf litter. Soil Biology and Biochemistry **54**:57-67.
Wallander, H., L. O. Nilsson, D. Hagerberg, and E. Bååth. 2001. Estimation of the biomass and seasonal growth of external mycelium of ectomycorrhizal fungi in the field. New Phytologist **151**:753-760.
Wallander, H., and G. Thelin. 2008. The stimulating effect of apatite on ectomycorrhizal growth diminishes after PK fertilization. Soil Biology and Biochemistry **40**:2517-2522.
Washbourne, C.-L., E. Lopez-Capel, P. Renforth, P. L. Ascough, and D. A. C. Manning. 2015. Rapid Removal of Atmospheric CO2 by Urban Soils. Environmental Science & Technology **49**:5434-5440.
Weissenhorn, I., P. Floris, and B. Nederland. 2002. Mycorrhiza and Salt Tolerance of Trees.
Weryszko-Chmielewska, E., K. Piotrowska-Weryszko, and A. Dąbrowska. 2019. Response of Tilia sp. L. to climate warming in urban conditions – Phenological and aerobiological studies. Urban Forestry & Urban Greening **43**:126369.
White, P. J., and M. R. Broadley. 2001. Chloride in Soils and its Uptake and Movement within the Plant: A Review. Annals of botany. **88**:967-988.
Wightwick, A. M., M. R. Mollah, D. L. Partington, and G. Allinson. 2008. Copper Fungicide Residues in Australian Vineyard Soils. Journal of Agricultural and Food Chemistry **56**:2457-2464.
Wu, P., A. Yin, M. Fan, J. Wu, X. Yang, H. Zhang, and C. Gao. 2018. Phosphorus dynamics influenced by anthropogenic calcium in an urban stream flowing along an increasing urbanization gradient. Landscape and Urban Planning **177**:1-9.
Zhou, X., H. Sun, J. Pumpanen, O.-M. Sietiö, J. Heinonsalo, K. Köster, and F. Berninger. 2019. The impact of wildfire on microbial C:N:P stoichiometry and the fungal-to-bacterial ratio in permafrost soil. Biogeochemistry **142**:1-17.
Zwiazek, J. J., M. A. Equiza, J. Karst, J. Senorans, M. Wartenbe, and M. Calvo-Polanco. 2019. Role of urban ectomycorrhizal fungi in improving the tolerance of lodgepole pine (Pinus contorta) seedlings to salt stress. Mycorrhiza **29**:303-312.

Acknowledgements

I wish to express my gratitude to the numerous people who made the completion of this project possible.

First and foremost, I would like to thank Dr. Hans Sandén and Dr. Boris Rewald, my supervisors on this project, for all their encouragement, guidance, and limitless patience, and for the comfortable learning environment they provided for me during this project.

Thank you to my colleague Vera Mayr for our enjoyable field work, and for the meetings and discussions that helped shape this study.

Thank you to the laboratory team at the Institute for Forest Ecology: Marcel Hirsch, Linda Fleck and Frauke Neumann for their help and advice with laboratory procedures I had never encountered before.

Thank you to Dr. Christoph Rosinger for the many informal chats, where my questions were often answered in great detail. Our conversations over coffee gave me much needed nudges in the right direction.

Finally, thank you to my wife Sinéad Harvey for her belief in me, for her patience, and for encouraging me to keep going until I got here.

Appendix

Enzymes

Fresh soil samples were analysed for soil enzyme activity within four days of sampling. One gram of soil per street tree was suspended in 100ml of buffer solution (100*mM* sodium acetate, pH 4.5) and was subsequently homogenised for 1 minute in a sonication bath. 200 µl of soil-buffer slurry was pipetted from containers stirred on a magnetic stir plate into black 96-well microplates. The sample suspension was mixed with the substrates by horizontal shaking for 30 seconds, after which the plates were sealed with film and stored in darkness at 20°C for 120 minutes.

Sample plates were designed to analyse 22 samples in each plate, with three replicates per sample (200µl soil slurry and 50 µl substrate) and one well as a standard well (200µl soil slurry and 25 µl universal buffer and 25 µl mub 250) to try to take the high heterogeneity of urban soils into account and create a quenching coefficient for each sample. Substrates used were: *ß*-glucosidase (GLU), leucine-aminopeptidase (LAP), N-acetyl-glucosaminidase (NAG), and Acid Phosphatase (AP), all purchased from Sigma Aldrich. One sample plate was prepared for each substrate (GLU, LAP, NAG, AP) with soil slurry and buffer to the same plate layout (Figure 1). A Perkin Elmer EnSpire multiplate reader (Perkin Elmer Inc., Waltham, Massachusetts, USA) was used to measure fluorescence.

FIGURE 1 ENZYME SAMPLE PLATE LAYOUT

For the standard curves, a separate standard plate was analysed with each batch of sample plates, using a soil slurry with medium hue (soil 1), a dark hue (soil 2) and a light hue (soil 3) chosen from the soils used for the sample plates in the same run in the multiplate reader. These soils were mixed with varying amounts of buffer solution and either 4-methylumbelliferone (MUB) or 7-amino-4-methylcoumarin (AMC) (Figure 2). This created a standard curve for each sample plate.

	1	2	3	4	5	6	7	8	9	10	11	12
A	Sample 200µl Substrate 50µl	Sample 200µl Substrate 50µl	Sample 200µl Substrate 50µl	Sample 200µl Substrate 50µl	Sample 200µl Substrate 50µl	Sample 200µl Substrate 50µl	Sample 200µl Substrate 50µl	Sample 200µl Substrate 50µl	Sample 200µl Substrate 50µl	Sample 200µl Substrate 50µl	Sample 200µl Substrate 50µl	Buffer 200µl Substrate 50µl
B	Sample 200µl Substrate 50µl	Sample 200µl Substrate 50µl	Sample 200µl Substrate 50µl	Sample 200µl Substrate 50µl	Sample 200µl Substrate 50µl	Sample 200µl Substrate 50µl	Sample 200µl Substrate 50µl	Sample 200µl Substrate 50µl	Sample 200µl Substrate 50µl	Sample 200µl Substrate 50µl	Sample 200µl Substrate 50µl	Buffer 200µl Substrate 50µl
C	Sample 200µl Substrate 50µl	Sample 200µl Substrate 50µl	Sample 200µl Substrate 50µl	Sample 200µl Substrate 50µl	Sample 200µl Substrate 50µl	Sample 200µl Substrate 50µl	Sample 200µl Substrate 50µl	Sample 200µl Substrate 50µl	Sample 200µl Substrate 50µl	Sample 200µl Substrate 50µl	Sample 200µl Substrate 50µl	Buffer 200µl Substrate 50µl
D	Sample 200µl Buffer 25µl Standard 25µl	Sample 200µl Buffer 25µl Standard 25µl	Sample 200µl Buffer 25µl Standard 25µl	Sample 200µl Buffer 25µl Standard 25µl	Sample 200µl Buffer 25µl Standard 25µl	Sample 200µl Buffer 25µl Standard 25µl	Sample 200µl Buffer 25µl Standard 25µl	Sample 200µl Buffer 25µl Standard 25µl	Sample 200µl Buffer 25µl Standard 25µl	Sample 200µl Buffer 25µl Standard 25µl	Sample 200µl Buffer 25µl Standard 25µl	Buffer 200µl Substrate 50µl
E	Sample 200µl Substrate 50µl	Sample 200µl Substrate 50µl	Sample 200µl Substrate 50µl	Sample 200µl Substrate 50µl	Sample 200µl Substrate 50µl	Sample 200µl Substrate 50µl	Sample 200µl Substrate 50µl	Sample 200µl Substrate 50µl	Sample 200µl Substrate 50µl	Sample 200µl Substrate 50µl	Sample 200µl Substrate 50µl	Buffer 250µl
F	Sample 200µl Substrate 50µl	Sample 200µl Substrate 50µl	Sample 200µl Substrate 50µl	Sample 200µl Substrate 50µl	Sample 200µl Substrate 50µl	Sample 200µl Substrate 50µl	Sample 200µl Substrate 50µl	Sample 200µl Substrate 50µl	Sample 200µl Substrate 50µl	Sample 200µl Substrate 50µl	Sample 200µl Substrate 50µl	Buffer 250µl
G	Sample 200µl Substrate 50µl	Sample 200µl Substrate 50µl	Sample 200µl Substrate 50µl	Sample 200µl Substrate 50µl	Sample 200µl Substrate 50µl	Sample 200µl Substrate 50µl	Sample 200µl Substrate 50µl	Sample 200µl Substrate 50µl	Sample 200µl Substrate 50µl	Sample 200µl Substrate 50µl	Sample 200µl Substrate 50µl	Buffer 250µl
H	Sample 200µl Buffer 25µl Standard 25µl	Sample 200µl Buffer 25µl Standard 25µl	Sample 200µl Buffer 25µl Standard 25µl	Sample 200µl Buffer 25µl Standard 25µl	Sample 200µl Buffer 25µl Standard 25µl	Sample 200µl Buffer 25µl Standard 25µl	Sample 200µl Buffer 25µl Standard 25µl	Sample 200µl Buffer 25µl Standard 25µl	Sample 200µl Buffer 25µl Standard 25µl	Sample 200µl Buffer 25µl Standard 25µl	Sample 200µl Buffer 25µl Standard 25µl	Buffer 250µl

	1	2	3	4	5	6	7	8	9	10	11	12
A	Buffer 250µl	Soil 1 200µl Buffer 50µl	Buffer 250µl	Soil 1 200µl Buffer 50µl	Soil 2 200µl Buffer 50µl	Soil 3 200µl Buffer 50µl	Buffer 250µl	Soil 1 200µl Buffer 50µl	Buffer 250µl	Soil 1 200µl Buffer 50µl	Buffer 250µl	Soil 1 200µl Buffer 50µl
B	Buffer 245µl 5µl mub 10	Soil 1 200µl Buffer 45µl 5µl mub 10	Buffer 245µl 5µl mub 20	Soil 1 200µl Buffer 45µl 5µl mub 20	Soil 2 200µl Buffer 45µl 5µl mub 20	Soil 3 200µl Buffer 45µl 5µl mub 20	Buffer 245µl 5µl mub 250	Soil 1 200µl Buffer 45µl 5µl mub 250	Buffer 245µl 5µl AMC 20	Soil 1 200µl Buffer 45µl 5µl AMC 20	Buffer 245µl 5µl AMC 50	Soil 1 200µl Buffer 45µl 5µl AMC 50
C	Buffer 240µl 10µl mub 10	Soil 1 200µl Buffer 40µl 10µl mub 10	Buffer 240µl 10µl mub 20	Soil 1 200µl Buffer 40µl 10µl mub 20	Soil 2 200µl Buffer 40µl 10µl mub 20	Soil 3 200µl Buffer 40µl 10µl mub 20	Buffer 240µl 10µl mub 250	Soil 1 200µl Buffer 40µl 10µl mub 250	Buffer 240µl 10µl AMC 20	Soil 1 200µl Buffer 40µl 10µl AMC 20	Buffer 240µl 10µl AMC 50	Soil 1 200µl Buffer 40µl 10µl AMC 50
D	Buffer 235µl 15µl mub 10	Soil 1 200µl Buffer 35µl 15µl mub 10	Buffer 235µl 15µl mub 20	Soil 1 200µl Buffer 35µl 15µl mub 20	Soil 2 200µl Buffer 35µl 15µl mub 20	Soil 3 200µl Buffer 35µl 15µl mub 20	Buffer 235µl 15µl mub 250	Soil 1 200µl Buffer 35µl 15µl mub 250	Buffer 235µl 15µl AMC 20	Soil 1 200µl Buffer 35µl 15µl AMC 20	Buffer 235µl 15µl AMC 50	Soil 1 200µl Buffer 35µl 15µl AMC 50
E	Buffer 230µl 20µl mub 10	Soil 1 200µl Buffer 30µl 20µl mub 10	Buffer 230µl 20µl mub 20	Soil 1 200µl Buffer 30µl 20µl mub 20	Soil 2 200µl Buffer 30µl 20µl mub 20	Soil 3 200µl Buffer 30µl 20µl mub 20	Buffer 230µl 20µl mub 250	Soil 1 200µl Buffer 30µl 20µl mub 250	Buffer 230µl 20µl AMC 20	Soil 1 200µl Buffer 30µl 20µl AMC 20	Buffer 230µl 20µl AMC 50	Soil 1 200µl Buffer 30µl 20µl AMC 50
F	Buffer 225µl 25µl mub 10	Soil 1 200µl Buffer 25µl 25µl mub 10	Buffer 225µl 25µl mub 20	Soil 1 200µl Buffer 25µl 25µl mub 20	Soil 2 200µl Buffer 25µl 25µl mub 20	Soil 3 200µl Buffer 25µl 25µl mub 20	Buffer 225µl 25µl mub 250	Soil 1 200µl Buffer 25µl 25µl mub 250	Buffer 225µl 25µl AMC 20	Soil 1 200µl Buffer 25µl 25µl AMC 20	Buffer 225µl 25µl AMC 50	Soil 1 200µl Buffer 25µl 25µl AMC 50
G	Buffer 220µl 30µl mub 10	Soil 1 200µl Buffer 20µl 30µl mub 10	Buffer 220µl 30µl mub 20	Soil 1 200µl Buffer 20µl 30µl mub 20	Soil 2 200µl Buffer 20µl 30µl mub 20	Soil 3 200µl Buffer 20µl 30µl mub 20	Buffer 220µl 30µl mub 250	Soil 1 200µl Buffer 20µl 30µl mub 250	Buffer 220µl 30µl AMC 20	Soil 1 200µl Buffer 20µl 30µl AMC 20	Buffer 220µl 30µl AMC 50	Soil 1 200µl Buffer 20µl 30µl AMC 50
H	Buffer 215µl 35µl mub 10	Soil 1 200µl Buffer 15µl 35µl mub 10	Buffer 215µl 35µl mub 20	Soil 1 200µl Buffer 15µl 35µl mub 20	Soil 2 200µl Buffer 15µl 35µl mub 20	Soil 3 200µl Buffer 15µl 35µl mub 20	Buffer 215µl 35µl mub 250	Soil 1 200µl Buffer 15µl 35µl mub 250	Buffer 215µl 35µl AMC 20	Soil 1 200µl Buffer 15µl 35µl AMC 20	Buffer 215µl 35µl AMC 50	Soil 1 200µl Buffer 15µl 35µl AMC 50

FIGURE 2 PLATE SETUP FOR STANDARD CURVE PLATES

Potential enzyme activity (nmol. g dry soil^{-1}.h^{-1}) was calculated using the following equations (German et al. 2011):

- Activity = [Net fluorescence x Buffer volume (ml)] / [Emission coefficient x Homogenate volume (ml) x Time (h) x Soil mass (g) x Dry mass factor]
- Net fluorescence = [(Assay – Homogenate control) – Quenching coefficient] – Substrate control
- Emission coefficient = Standard curve slope [Fluorescence / nmol / ml] / Assay volume (ml)
- Quenching coefficient = [Slope of Standard curve (in presence of homogenate)] / [Slope of Standard curve (in presence of buffer)]

Soil Cations

Location	Number	Ca mg/g	Cd ug/g	Cu ug/g	K mg/g	Mg mg/g	Na ug/g	P ug/g
Park	26		0.0065	0.4843	0.2696	0.2219	78.7299	35.2871
Park	27	5.658	0.0086	0.6225	0.3298	0.2893	43.9671	59.3158
Park	28	5.5431	0.0141	1.1569	0.4686	0.1818	23.3308	61.3475
Park	32	5.6158	0.0033	0.4836	0.1958	0.2422	23.6196	40.1168
Park	77	6.4599	0.0313	0.675	0.18	0.2751	26.304	12.6474
Park	79	5.8779	0.0239	0.898	0.1737	0.2302	40.6386	20.1028
Park	80	5.8956		1.1553	0.2055	0.2841	49.7682	34.4629
Park	81	6.6063	0.0033	0.8138			49.0769	77.8086
Park	98	6.5438	0.0033	0.4099	0.2262	0.3402	32.4563	11.6608
Park	99	6.5428	0.0033	0.6586	0.306	0.3241	25.0996	17.8327
Park	100	6.4048	0.0033	0.5649	0.3785	0.3726	37.0765	12.8944
Park	101	6.6164	0.0033	0.4396	0.1953	0.3459	36.8822	8.7272
Park	102	6.1564	0.0033	0.8256	0.4005	0.3336	38.8457	27.1926
Park	103	6.7748	0.0033	0.7934	0.2422	0.2689	29.0354	58.0298
Park	112		0.013	0.6075	0.4582	0.3186		62.1362
Park	114	5.595	0.0095	0.8479	0.259	0.2211	31.5985	54.0865
Park	115	6.5077	0.0033		0.1642	0.2726	32.8816	18.7422
Park	116	5.8105	0.0033		0.2427	0.2179	33.3056	58.2306
Park	117	6.0773	0.0084	1.0483	0.1732	0.2071	31.0523	34.6378
Side	52	5.5627	0.0033	0.574	0.2799	0.1762	45.6469	44.72
Side	53	5.3405	0.0033	0.4861	0.3344	0.2529	43.9204	79.5037
Side	54	5.2673	0.0033	0.6842	0.2654	0.2159	71.6777	86.7816
Side	55	5.4345	0.0051	0.5489	0.1442	0.1647	52.7437	28.7737
Side	56	5.7986	0.0089	0.475	0.1929	0.1027	75.2011	12.2155
Side	57	5.2863	0.0072	0.453	0.2303	0.1393		19.6497
Side	58	6.6436	0.0033	0.6661	0.2338	0.2113	243.0833	16.6455
Side	63	6.1488	0.0033	0.6063	0.1964	0.2588	45.3926	64.7742
Side	64	6.5852		0.8306	0.2501	0.2421	83.6714	46.0652
Side	65	5.9811	0.0251	0.6738	0.1777	0.2266	75.2741	49.584
Side	66	5.8608	0.0033	0.4758	0.1602	0.2228	99.254	
Side	71	4.9589	0.0033	0.3226	0.2366	0.1523	50.9922	59.6833
Side	72	5.7519	0.0033	0.3973	0.2978	0.1735	37.4519	20.4286
Side	73	5.8591	0.0033	0.4513	0.2752	0.2244	50.5543	35.1058
Side	86	6.1009	0.0342	0.5732		0.2526	183.2607	25.957
Side	87	5.9934	0.0059	0.4697	0.2419	0.1761	25.9968	8.7625
Side	88	5.9238	0.0033	0.5111	0.2726	0.1809	32.9795	15.5332
Side	89	6.1942	0.0072	0.4917	0.1425	0.2078	51.394	8.8991
Side	93		0.054	0.8318	0.164	0.2954	100.5562	17.4354
Side	94		0.0209	0.7562	0.2117		211.1935	44.5322
Main	37		0.0033	0.3158	0.2609	0.4116	185.6102	8.4296
Main	38	5.4875	0.0406	0.6736	0.1904	0.3472	138.2903	15.1556
Main	39		0.0033	0.305	0.1789		159.1309	30.1423
Main	46	6.3251	0.0215	0.6112	0.1272	0.1038	34.343	24.5204
Main	47	6.0865	0.0151	0.7805	0.1876	0.1297	28.1065	16.4228
Main	48	6.5859	0.0033	0.6078	0.2186	0.2537	33.6666	27.5326
Main	67	5.1768	0.0033	0.4651	0.14	0.1155	61.2896	22.844
Main	68	6.6615	0.0072	0.7097	0.1622	0.175	47.3299	50.772
Main	69	5.9097	0.0065	0.691	0.221	0.1438	78.6896	22.5679
Main	74	5.2054	0.0405		0.182	0.1585	95.6528	39.1369
Main	75	5.6822	0.0033	0.8038	0.3315	0.1698	83.0806	
Main	76	6.005	0.0157	0.9677	0.3089	0.1921	43.6081	46.1341
Main	90	5.2732	0.0196	0.5942	0.4135	0.1749	303.148	19.179
Main	91	5.6409	0.0241	0.7522	0.3846	0.1916	191.8167	26.8232
Main	92	5.575		0.6903	0.3529	0.1859		26.3809
Main	107	6.9867	0.0172	0.592	0.1479	0.2751	113.5545	25.2923